

1 Future snowfall in the Alps: Projections based on the EURO- 2 CORDEX regional climate models

3 Prisco Frei, Sven Kotlarski, Mark A. Liniger, Christoph Schär

6 - Response to Referees -

8 General

9 We thank the three referees for their careful revision of the manuscript and for their constructive comments.
10 Please find below our replies to all major comments and our suggestions on how to address these issues in a
11 revised manuscript. We hope that we satisfactorily addressed all referee comments and that the proposed
12 changes are considered as being appropriate. In case that not, we'd be looking forward to discuss individual
13 remaining issues in more detail.

14 As several referee comments addressed the RCM evaluation and the evaluation of the 2 km snowfall reference
15 itself, we'd like to put in front the following two statements on the scope of the paper:

16
17 (1) Our work is primarily concerned with the analysis of future snowfall projections. However, a basic notion on
18 the quality of raw RCM snowfall and, hence, the general ability of RCMs to represent our variable of interest is
19 required for such an exercise in our opinion. In the manuscript this is accomplished by comparing RCM raw
20 snowfall against site-scale measurements obtained from new snow sums (Figure 3). Such a comparison is
21 subject to considerable uncertainties, mostly originating from the scale gap between RCM grid cells and site-scale
22 observations and from representativity issues of observed snow cover. Due to a missing high-quality
23 observational reference at the scale of the RCM resolution (in our opinion also the HISTALP dataset has its
24 shortcomings; see below) we refrain from evaluating RCM snowfall in more detail and, at least when interpreting
25 raw snowfall change signals, implicitly assume stationary model biases. As a consequence, the projection aspect
26 of the current work is much larger than the evaluation aspect, and we tried to better clarify this issue by modifying
27 the text in Chapters 1 and 3.1. Furthermore, we adjusted the title of the manuscript accordingly and removed the
28 term "Evaluation".

29
30 (2) Relating to the previous issue but especially to the validation of the snowfall reference against which the RCM-
31 derived snowfall is adjusted: As it was already mentioned in the introduction of the original manuscript, we do not
32 claim to present an ultimate solution for bias-adjusting RCM-based snowfall but employ a spatially and temporally
33 aggregated adjustment procedure that does nevertheless separately account for temperature and precipitation
34 biases. Aspects of the snowfall climate that are not corrected for, such as details of the spatial snowfall pattern,
35 are described in Sections 2.6 and 3.3. The simplifications also include the fact that we basically accept a non-
36 perfect observation-based reference. A well-validated and appropriate reference does not exist in our opinion (see
37 also above). The very core of our work is the analysis of projected future snowfall changes and the comparison of
38 three different ways to produce such estimates: (1) Raw RCM snowfall, (2) RCM snowfall as separated from
39 simulated temperature and precipitation, and (3) RCM snowfall as separated from simulated temperature and
40 precipitation and additionally bias-adjusted. The latter version is the basic dataset for the climate scenario
41 analysis as it can be constructed for all participating RCMs (raw snowfall is not available for all of them) and as it
42 is, in principle, able to account for temperature-dependent and hence non-stationary snowfall biases. However,
43 Chapter 5.3 shows that relative change estimates largely agree among all three datasets and are robust. From
44 that point of view, the influence of remaining inaccuracies in the bias-adjusted snowfall projections due to
45 inaccuracies of the reference is presumably small. In the revised version we now try to better clarify these issues
46 by modifying Chapters 1, 2.5, 2.6 and 5.3.

48 Response to Referee #2

49 **Comment** *First of all, in absence of a daily observational gridded snowfall dataset for the Alpine region the authors derive a dataset using daily
50 temperatures and precipitation. They separate the snow fraction from the total precipitation using a fixed temperature threshold $T^*=2$ C. While this
51 method works fine with hourly data, it is probably weak when using data at daily scale. As the rest of the paper builds on the hypothesis that this
52 snowfall dataset represents the ground truth (i.e. the hypothesis is used for the calculation of Richardson snowfall fraction f_s, R_i ; for the bias
53 correction of RCM snowfall fields) authors should provide some evidence that their snowfall dataset closely represent the real snowfall distribution.*

54 **Response and changes to manuscript** We are thankful for this comment. It relates to a detail of the manuscript
55 where (1) we might have been misunderstood when laying out the scope and the objectives of the work, but
56 where also (2) a proper comparison to other datasets was obviously missing. Please see our comments in the
57 introduction of these replies concerning the scope and objectives of the work. In the revised manuscript we now
58 try to make the point clear that our climate scenario assessment is, in the end, based on three different snowfall
59 datasets that differ with respect to if and how the climate model data were postprocessed. Chapter 5.3 of the

60 manuscript inter-compares the three approaches and concludes that at least for relative change signals the
61 results are robust and do only slightly depend on the postprocessing strategy that is applied. The observation-
62 based snowfall reference grid is used in two of these approaches, but not in the assessment based on raw RCM
63 snowfall. The fact that all three estimates basically agree with each other in terms of relative change signals
64 (which are the core of the paper) downweights the importance of the reference dataset for snowfall separation
65 and bias-adjustment, and we can accept an only approximate reproduction of the (unknown) real snowfall climate.
66 Concerning the evaluation of the reference snowfall grid the new manuscript version now includes a comparison
67 to station-based fresh snow sums as well as a comparison to the HISTALP product. These additional analyses
68 are part of the new sub-Chapter 3.2 "Evaluation of the reference snowfall". Please see the replies below for
69 further details. We hope these changes to the manuscript are considered appropriate.

70 **Comment** *In the Results (section 3.1) it comes really unexpected that the authors validate the RCM raw snowfall outputs by using 29 fresh-snow*
71 *daily time series from MeteoSwiss stations. This dataset was not presented before and should be described in the "Observational datasets"*
72 *section. Moreover this datasets is by definition "the" ground-truth, and I wonder why it comes out only at this point. It should be used for a detailed*
73 *validation of the 2 km gridded snowfall product that you derive from temperature and precipitation fields. How the 2km gridded product compares*
74 *to the fresh snow observations? Does it represent properly the snowfall climatology (mean, extremes) in correspondence of the stations? Does it*
75 *represent the altitudinal gradient of mean/extreme snowfalls intensities? This information on the quality of the gridded reference dataset should be*
76 *provided as it is necessary to set the basis for the whole methodology.*

77 **and**

78 **Comment** *Finally the RCM bias correction methods is calibrated on the area of Switzerland only and then applied to the whole Alpine region. This*
79 *is justified by the authors with the lack of information on snowfall beyond the borders of Switzerland. Indeed previous efforts were made to derive a*
80 *gridded snowfall dataset for the Alpine Region: HISTALP dataset provides monthly snowfall over the full Alpine domain, since 1800, at about 10*
81 *km spatial resolution, i.e. resolution comparable to the RCM gridsize (12 km). I believe this manuscript should include the HISTALP dataset in the*
82 *analysis, in order to provide a comprehensive view on the reference datasets. In particular I would suggest to discuss i) how HISTALP compares*
83 *with the stations and the 2km gridded dataset in the Swiss Alps; ii) if it is a good quality reference for validating the RCM snowfall outputs at*
84 *monthly (or longer) time scales over the Swiss domain.*

85 **Response and changes to manuscript** Thank you very much for these detailed suggestions on improving the
86 manuscript. We agree that a quality assessment of our 2 km snowfall reference has been missing so far. At the
87 same time, however, a comparison against the station-based fresh snow sums is subject to considerable
88 uncertainties as well (see our comments in the beginning of these replies and the new text section in Chapter
89 3.1). Furthermore, the bias-adjusted RCM snowfall (adjusted against the aggregated 2 km reference) is only one
90 out of three estimates used for the snowfall projections. The three estimates yield rather similar results in terms of
91 relative snowfall changes, which downweights the relevance of the specific reference used.

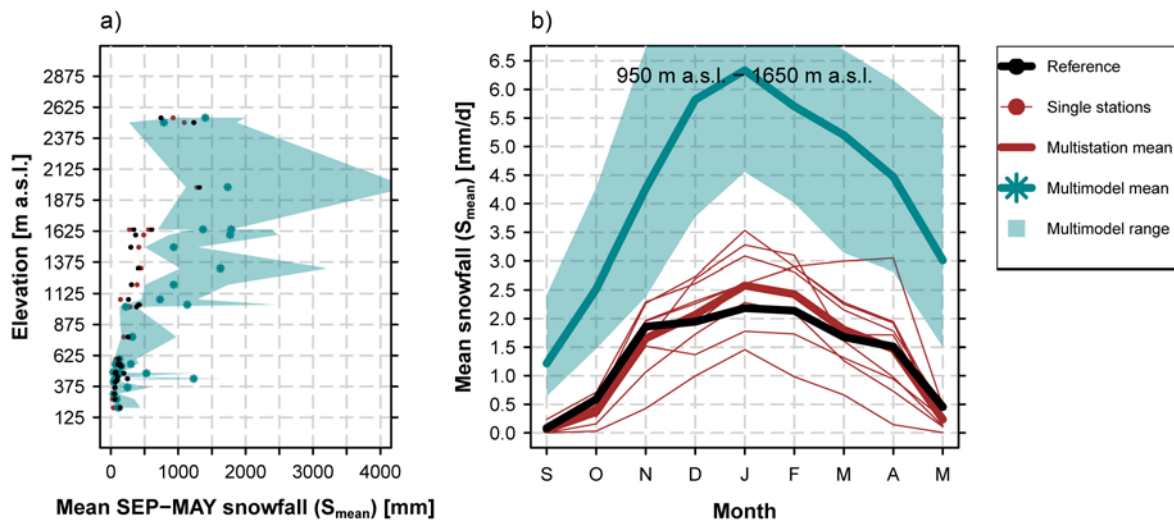
92 Altogether, we still agree that some quality assessment of the reference is helpful. For this purpose we introduced
93 a new sub-Chapter 3.2 "Evaluation of reference snowfall". This sub-Chapter includes a modification to the existing
94 Figure 3 (additional comparison of the reference against the new snow observations at stations in terms of the
95 mean snowfall climate) and a new supplementary Figure S5 (comparison against the monthly HISTALP dataset).
96 Regarding the suggested evaluation of individual grid cells of the 2km gridded snowfall reference against the
97 fresh snow sums at stations we refrain from including this analysis at a prominent place in the paper as little can
98 be learned due to the remaining scale gap (2 km grid cells vs. site scale) and the problem of non-representativity
99 of snow depth measurements in topographically structured terrain (see new text in Chapter 3.1). For your
100 information, we however present this analysis in Figure R1 below. Despite the inherent uncertainties of the
101 intercomparison, the 2 km snowfall reference and the site observations agree fairly well with each other in terms
102 of climatological mean snowfall. This basic information is now also provided in the manuscript (Chapter 3.2)
103 though without showing the figure.

104

105

106

107



108
 109 **Figure R1:** As Figure 3 of the revised manuscript but for the simulated data (green) and for the 2 km snowfall reference (black)
 110 only those grid cells that directly cover the 29 MeteoSwiss stations are considered.

111
 112 Concerning the evaluation against HISTALP, a comparison of the 2 km reference as well as of the reference on
 113 the RCM grid (after applying the Richards equation) yields an approximate agreement. However, due to the
 114 method used to construct the HISTALP solid precipitation grid (application of monthly snowfall fraction factors to a
 115 spatially interpolated total precipitation grid) and the comparatively coarse station network considered for the total
 116 precipitation grid (192 stations) we believe that also the HISTALP reference is subject to considerable
 117 uncertainties and only a qualitative comparison is valid. The strength of HISTALP clearly lies in the long period
 118 covered, but not necessarily in spatial detail at high (daily) temporal resolution.

119 Following your suggestion, we now also introduce the station-based fresh snow sum dataset in Chapter 2.1.

120 **Comment P 7 L254:** “We apply this regression to relate the surface temperature T to the snow fraction f_s by accounting for the topographic
 121 subgrid variability. At each coarse gridpoint k , the Richards method-based snowfall fraction $f_{s,RI}$ for a given day is hence computed as follows ...
 122 First, we estimate the two parameters C and D of Equation 4 for each single coarse grid point k by minimizing the least-square distance to the f_s
 123 values derived by the Subgrid method via the reference snowfall SSG (local fit).”

124 *The method used to separate snowfall with the temperature threshold $T^*=2\text{ C}$ is effective with hourly data but it is crude when using daily data as it
 125 returns snowfall fraction $f_s=1$ or $f_s=0$ in a given day. This can be far from the reality, especially at middle elevations (throughout the snow season)
 126 but also at high elevations in spring and autumn. The $f_{s,RI}$ depends on the C and D , and the latter are estimated assuming that f_s is a good
 127 estimator of the solid precipitation fraction. But as said above f_s is characterized by unknown uncertainty. You should prove that f_s closely
 128 reproduce the real snowfall fraction, before applying your method for deriving $f_{s,RI}$ and your snowfall reference dataset. Minimum requirement is
 129 to provide a quantification of this error, using fresh snow manual observations in the 29 manual stations.*

130 **Response and changes to manuscript** Please see our replies above and at the beginning of the replies section.
 131 The 2 km reference snowfall grid is now approximately evaluated. However, your concerns are certainly right. Any
 132 binary method based on near-surface air temperature can only be an approximation of true snowfall. further
 133 presumably more accurate methods are listed by Steinacker (2013). But note that binary methods on daily scales
 134 are frequently used in the literature to separate snowfall from total precipitation, for instance in the hydrological
 135 and glaciological modelling community. A further example cited in the manuscript is the work of Zubler et al.
 136 (2014) who applied the same binary separation at a temperature threshold of 2°C .

137 **Comment P9 L317-321:** “the initial snow fractionation temperature $T^*=2\text{ C}$ of the Richards separation method (see Sec 2.5) is shifted to the value
 138 T^*a for which the spatially and temporally averaged simulated snowfall amounts for elevations below 2750 m a.s.l. match the respective
 139 observation-based reference.”

140 *With this temperature correction you basically report the RCM snowfall to your reference. So, also in this case, before applying this procedure you
 141 need an evaluation of the error on your snowfall reference. Moreover, can you give details on how you calculate spatial and temporal averages,
 142 i.e. which domain/ time range?*

143 **Response and changes to manuscript** Concerning the evaluation of the snowfall reference please see our
 144 replies above. Regarding the domain and time range, this information was actually provided two sentences
 145 afterwards (Swiss domain and September to May). In the revised manuscript we moved this information to the
 146 sentence you are referring to.

147 **Comment P9 L327:** “Note that, as the underlying high-resolution data sets are available over Switzerland only, the calibration of the bias
 148 correction methodology is correspondingly restricted, but the correction is then applied to the whole Alpine domain.” HISTALP dataset provides
 149 gridded snowfall monthly fields for the Alpine region at about 10 km spatial resolution (Chimani et al 2011), it should be included in the analysis
 150 and discussed in comparison to your reference/manual observations in Switzerland: Chimani, B., Böhm R., Matulla C., Ganekind M.: Development
 151 of a longterm dataset of solid/liquid precipitation Adv.Sci.Res,6,39-43, 2011http://www.adv-scires.net/6/39/2011/asr-6-39-2011.html

152 **Response and changes to manuscript** Please see our replies above. HISTALP is now used to approximately
153 validate both the 2 km and the 0.11° snowfall reference. The paper of Chimani et al. is cited now. Thanks for
154 pointing us to this dataset (of which we have not been aware)!

155 **Comment P10 L338-341:** "EURO-CORDEX simulations ... are compared against observations derived from measured fresh snow sums from 29
156 Meteo Swiss stations with data available for at least 80% of the evaluation period. For this purpose a mean snow density of 100 kg/m³ for the
157 conversion from measured snow height to water equivalent is assumed."
158

159 *As said before, I am surprised to see at this point of the paper that you have 29 fresh snowfall time series covering the 1970-2005 period. They
160 should be presented before (section 3.1) & exploited much more than you do. These manned observations are the ground truth and they should
161 be used to validate the snowfall gridded dataset that you derive from temperature and precipitation over Switzerland. Please provide a quality
162 control of the snowfall gridded dataset prior to use it*

163 **Response and changes to manuscript** Please see our replies above. The comparison against fresh snow sums
164 can only be of approximate nature and is subject to large uncertainties. See the additional text in Chapter 3.1.
165 We'd refrain from considering these data as the "ground truth". These data are now introduced in Chapter 2.1
166 along with gridded observational data. They are also employed to approximately validate the 2 km and 0.11°
167 snowfall reference grid.

168 **Comment P10 L345-347:** "The positive bias at high elevations might arise from the fact that the very few observations were made at a specific
169 location while simulated grid point values of the corresponding elevation interval might be located in different areas of Switzerland." Here you
170 consider all Switzerland and you really mix very different areas far away one from another. Please discuss the case when only the gridpoints
171 containing stations are considered, i.e. showing the spread of the models around the observed time series (i.e. in plots for the three - low, middle
172 and high - elevation ranges?)

173 **Response and changes to manuscript** Please see our replies above and Figure R1. In our opinion such a
174 comparison is subject to large uncertainties, mainly due to the mismatch of spatial representativeness between an
175 individual grid cell and an individual site. By design, such an evaluation can only be of approximate nature. See
176 also the additional text in Chapter 3.1 on the limitations of such a comparison. In our opinion, averaging over
177 elevation intervals and showing the respective spread (which covers or does not cover the site-scale
178 observations) is clearly the safer option.

179 **Comment P14 L487:** "In between is a transition zone with rather strong changes with elevation". Can you explain why?

180 **Response and changes to manuscript** This transition approximately corresponds to the mean elevation of the
181 SEP-MAY zero-degree line in today's climate. We added this information to the manuscript plus two additional
182 references. Elevations close to this line seem to be especially sensitive, which is in line with previous works
183 addressing future snow cover changes.

184 **Comment P14 L494-6:** Could it also be residual biases along the snowfall line?

185 **Response and changes to manuscript** We do not think so, as further analyses (see above; comparison of the
186 three approaches) indicate a robust relative climate change signal also at low elevations, no matter if raw (and
187 hence biased), separated or separated + bias-adjusted snowfall is analyzed.

188 **Comment P16 L587-8:** Given more precipitation at high elevation & temperatures more favorable to heavy snowfalls, why does the snowfall
189 frequency decrease?

190 **Response and changes to manuscript** This is explained in the brackets at the end of this sentence: The light
191 grey range (which is now explicitly mentioned in the caption of Figure 11) represents the temperature interval
192 below 2°C, i.e. approximately the interval where snowfall occurs at all (neglecting subgrid-scale effects and
193 assuming a binary threshold). Due to the general shift of the temperature distribution to the right (to higher
194 temperatures) the fraction underneath the red curve (scenario period) that falls into this interval is much smaller
195 than the one underneath the blue curve (control climate). This is equivalent to a decrease of the total snowfall
196 frequency, despite potential precipitation increases and higher mean snowfall intensities.

197 **Further technical corrections**

198 **Response and changes to manuscript** Thank you very much for these additional comments and ideas. All
199 suggested further technical corrections were implemented with the exception of: (1) P3 L79 "low" to "lower" (which
200 is not meaningful in our opinion), (2) suggested changes to Figure 6 (an important point here is the differing
201 spatial distribution of mean snowfall, this would not be apparent in figures of anomaly wrt. the reference), (3) P8
202 L280 (the respective text section refers to the Richards method, here the spread is indeed +/- 0.1 at maximum)
203 and (4) Figure 11 (this figure is schematic only, low and high elevations are not defined in detail).

204

205

206 **Further changes to the manuscript**

207 **Chapter 2.1 “Observational data”** For reasons of completeness we additionally included the information that the
208 temperature and precipitation grids employed are slightly shifted with respect to their reference time interval
209 (midnight UTC - midnight UTC for temperature, 06 UTC - 06 UTC for precipitation).

210 **Chapter 2.2 “Climate model data”** In the last paragraph we erroneously spoke of *six* RCMs considered. We
211 corrected this to *seven* RCMs.

212 **Chapter 3.1** To better account for uncertainties in this simplified evaluation we now additionally cite the work of
213 Grünewald and Lehning (2015) that highlights the danger of non-representativity of single-site snow depth
214 observations in Alpine terrain.

215 **Figure 3** In the left panel two of the 29 stations employed (WFJ and MVE) were plotted at a wrong elevation in
216 the original version. For both stations the correct elevation differs by about 100 m from the previously used
217 elevation. The figure has been corrected accordingly, in addition to the modifications to this figure mentioned
218 above. The conclusions of the analysis do not change.

219 **Overall manuscript** Several minor spelling and wording mistakes as well as an inconsistent use of past and
220 present tense were corrected.

221

222

223

Future sSnowfall in the Alps: ~~Evaluation~~ and pProjections based on the EURO-CORDEX regional climate models

Prisco Frei¹, Sven Kotlarski^{2,*}, Mark A. Liniger², Christoph Schär¹

¹ Institute for Atmospheric and Climate Sciences, ETH Zurich, [CH-8006](#), Zurich, Switzerland

² Federal Office of Meteorology and Climatology, MeteoSwiss, [CH-8058](#) Zurich-Airport, Switzerland

* Corresponding author: sven.kotlarski@meteoswiss.ch

Abstract. Twenty-first century snowfall changes over the European Alps are assessed based on high-resolution regional climate model (RCM) data made available through the EURO-CORDEX initiative. Fourteen different combinations of global and regional climate models with a target resolution of 12 km, and two different emission scenarios are considered. As raw snowfall amounts are not provided by all RCMs, a newly developed method to separate snowfall from total precipitation based on near-surface temperature conditions and accounting for subgrid-scale topographic variability is employed. The evaluation of the simulated snowfall amounts against an observation-based reference indicates the ability of RCMs to capture the main characteristics of the snowfall seasonal cycle and its elevation dependency, but also reveals considerable positive biases especially at high elevations. These biases can partly be removed by the application of a dedicated RCM bias correction-adjustment that separately considers temperature and precipitation biases.

Snowfall projections reveal a robust signal of decreasing snowfall amounts over most parts of the Alps for both emission scenarios. Domain and multi-model-mean decreases of mean September-May snowfall by the end of the century amount to -25% and -45% for RCP4.5 and RCP8.5, respectively. Snowfall in low-lying areas in the Alpine forelands could be reduced by more than -80%. These decreases are driven by the projected warming and are strongly connected to an important decrease of snowfall frequency and snowfall fraction and are also apparent for heavy snowfall events. In contrast, high-elevation regions could experience slight snowfall increases in mid-winter for both emission scenarios despite the general decrease of the snowfall fraction. These increases in mean and heavy snowfall can be explained by a general increase of winter precipitation and by the fact that, with increasing temperatures, climatologically cold areas are shifted into a temperature interval which favours higher snowfall intensities. In general, percentage changes of snowfall indices are robust with respect to the RCM postprocessing strategy employed: Similar results are obtained for raw, separated and separated + bias-adjusted snowfall amounts. Absolute changes, however, can differ among these three methods.

262 1 Introduction

263 Snow is an important resource for the Alpine regions, be it for tourism, hydropower generation, or
264 water management (Abegg et al., 2007). According to the Swiss Federal Office of Energy (SFOE)
265 hydropower generation accounts for approximately 55% of the Swiss electricity production (SFOE,
266 2014). Consideration of changes in snow climatology needs to address aspects of both snow cover
267 and snow-fall. In the recent past, an important decrease of the mean snow cover depth and duration in
268 the Alps was observed (e.g, Laternser and Schneebeli, 2003; Marty, 2008; Scherrer et al., 2004).
269 ~~Future p~~Projections of future snow cover changes based on using climate model simulations ~~of the~~
270 ~~anthropogenic greenhouse effect~~ indicate a further substantial reduction (Schmucki et al., 2015a;
271 Steger et al., 2013), strongly linked to the expected rise of temperatures (e.g., CH2011, 2011; Gobiet
272 et al., 2014). On regional and local scales rising temperatures exert a direct influence on snow cover in
273 two ways: First, total snowfall sums are expected to decrease by a ~~decreasing-lower~~ probability for
274 precipitation to fall as snow implying and a decreasing snowfall fraction (ratio between solid and total
275 precipitation). Second, snow on the ground is subject to faster and accelerated melt. These warming-
276 induced trends might be modulated by changes in atmospheric circulation statistics~~patterns~~.

277 Although the snowfall fraction is expected to decrease ~~at lower elevations~~ during the 21st century
278 (e.g., Räisänen, 2016), extraordinary snowfall events can still leave a trail of destruction. A recent
279 example was the winter 2013/2014 with record-breaking heavy snowfall events along the southern rim
280 of the European Alps (e.g., Techel et al., 2015). The catastrophic effects of heavy snowfall range from
281 avalanches and floods to road or rail damage. In extreme cases these events can even result in the
282 weight-driven collapse of buildings or loss of human life (Marty and Blanchet, 2011). Also mean
283 snowfall conditions, such as the mean number of snowfall days in a given period, can be of high
284 relevance for road management (e.g. Zubler et al., 2015) or airport operation. Projections of future
285 changes in ~~the snowfall-climate~~, including mean and extreme conditions, are therefore highly relevant
286 for long-term planning and adaptation purposes in order to assess and prevent related socio-economic
287 impacts and costs.

288 21st century climate projections typically rely on climate models. For large-scale projections, global
289 climate models (GCMs) with a rather coarse spatial resolution of 100 km or more are used. ~~For~~
290 assessing~~To assess~~ regional to local scale impacts, where typically a much higher spatial resolution
291 ~~of the projections~~ is required, a GCM can be dynamically downscaled by nesting a regional climate
292 model (RCM) over the specific domain of interest (Giorgi, 1990). In such a setup, the GCM provides
293 the lateral and sea surface boundary conditions to the RCM. One advantage of climate models is the
294 ability to estimate climate change in a physically based manner under different greenhouse gas (GHG)
295 emission scenarios. With the Intergovernmental Panel on Climate Change's (IPCC) release of the Fifth
296 Assessment Report (AR5; IPCC, 2013) the so-called representative concentration pathway (RCP)
297 scenarios have been introduced (Moss et al., 2010) which specify GHG concentrations and
298 corresponding emission pathways for several radiative forcing targets. To estimate inherent projection
299 uncertainties, ensemble approaches employing different climate models, different greenhouse gas
300 scenarios, and/or different initial conditions are being used (e.g., Deser et al., 2012; Hawkins and
301 Sutton, 2009; Rummukainen, 2010).

302 Within the last few years several studies targeting the future global and European snowfall evolution
303 based on climate model ensembles were carried out (e.g., de Vries et al., 2013; de Vries et al., 2014;
304 Krasting et al., 2013; O’Gorman, 2014; Piazza et al., 2014; Räisänen, 2016; Soncini and Bocchiola,
305 2011). Most of these analyses are based on GCM output or older generations of RCM ensembles at
306 comparatively low spatial resolution, which are not able to properly resolve snowfall events over
307 regions with complex topography. New generations of high resolution RCMs are a first step toward an
308 improvement on this issue. This is in particular true for the most recent high-resolution regional climate
309 change scenarios produced by the global CORDEX initiative (Giorgi et al., 2009) and its European
310 branch EURO-CORDEX (Jacob et al., 2014). The present work aims to exploit this recently
311 established RCM archive with respect to future snowfall conditions over the area of the European
312 Alps. It thereby complements the existing works of Piazza et al. (2014) and de Vries et al. (2014) who
313 among others also exploit comparatively high-resolved RCM experiments (partly originating from
314 EURO-CORDEX as well) but with a reduced ensemble size and/or not specifically targeting the entire
315 Alpine region.

316 In general and on decadal to centennial time scales, two main drivers of future snowfall changes over
317 the European Alps with competing effects on snowfall amounts are apparent from the available
318 literature: (1) Mean winter precipitation is expected to increase over most parts of the European Alps
319 and in most EURO-CORDEX experiments (e.g., Rajczak et al., in prep.; Smiatek et al., 2016) which in
320 principle could lead to higher snowfall amounts. (2) Temperatures are projected to considerably rise
321 throughout the annual cycle (e.g., Gobiet et al., 2014; Smiatek et al., 2016; Steger et al., 2013) with
322 the general effect of a decreasing snowfall frequency and fraction, thus potentially leading to a
323 reduction in overall snowfall amounts. Separating the above two competing factors is one of the
324 targets of the current study. A potential complication is that changes in daily precipitation frequency
325 (here events with precipitation > 1 mm/day) and precipitation intensity (average amount on wet days)
326 can change in a counteracting manner (e.g., Fischer et al., 2015; Rajczak et al., 2013), and that
327 relative changes are not uniform across the event category (e.g. Ban et al., 2015; Fischer and Knutti,
328 2016).

329 We here try to shed more light on these issues by addressing the ~~By covering both model evaluation~~
330 ~~and high-resolution future snowfall projections we are addressing the~~ following main objectives:

331 **Snowfall separation on an ~~(coarse resolution)~~ RCM grid.** Raw snowfall outputs are not available
332 for all members of the EURO-CORDEX RCM ensemble ~~and, furthermore, a gridded observational~~
333 ~~snowfall product that could serve as reference for RCM evaluation does not exist.~~ Therefore, an
334 adequate snowfall separation technique, i.e., the derivation of snowfall amounts based on readily
335 available daily near-surface air temperature and precipitation data, is required. Furthermore, ~~as the~~
336 ~~observational and simulated grids of the two latter variables are typically not available at the same~~
337 ~~horizontal resolution,~~ we seek for a snowfall separation method that accounts for the topographic
338 subgrid-scale variability of snowfall on the the coarser (RCM) grid.

339 **Snowfall bias correction adjustment.** Even the latest generation of RCMs is known to suffer from
340 systematic model biases (e.g., Kotlarski et al., 2014). In GCM-driven setups as employed within the

341 present work these might partly be inherited from the driving GCM. To remove such systematic model
342 biases in temperature and precipitation, a simple bias ~~correction-adjustment~~ methodology ~~is~~ will be
343 developed and employed in the present work. To assess its performance and applicability, different
344 snowfall indices in the bias-~~corrected-adjusted~~ and not bias-~~corrected-adjusted~~ output ~~are~~ will be
345 compared against observation-~~based~~ estimates.

346 **Snowfall projections for the late 21st century.** Climate change signals for various snowfall indices
347 over the Alpine domain and for specific elevation intervals, derived by a comparison of 30-year control
348 and scenario periods, ~~are will be~~ analysed under the assumption of the RCP8.5 emission scenario. In
349 addition, we aim to identify and quantify the main drivers of future snowfall changes and, in order to
350 assess emission scenario uncertainties, compare RCP8.5-based results with experiments assuming
351 the more moderate RCP4.5 emission scenario. Snowfall projections are generally based on three
352 different datasets: (1) raw RCM snowfall where available, (2) RCM snowfall separated from simulated
353 temperature and precipitation, and (3) RCM snowfall separated from simulated temperature and
354 precipitation and additionally bias-adjusted. While all three estimates are compared for the basic
355 snowfall indices in order to assess the robustness of the projections, more detailed analyses are
356 based on dataset (3) only.

357 In addition and as preparatory analysis, we carry out a basic evaluation of RCM-simulated snowfall
358 amounts. This evaluation, however, is subject to considerable uncertainties as a high-quality
359 observation-based reference at the required spatial scale is not available, and the very focus of the
360 present work is laid on the snowfall projection aspect.

361 ~~On centennial time scales, two main drivers of future snowfall changes over the European Alps with~~
362 ~~competing effects on snowfall amounts are apparent: (1) Mean winter precipitation is expected to~~
363 ~~increase over most parts of the European Alps and in most EURO-CORDEX experiments (e.g.,~~
364 ~~Rajczak et al., in prep.; Smiatek et al., 2016) which in principle could lead to higher snowfall amounts.~~
365 ~~(2) Temperatures are projected to considerably rise throughout the annual cycle (e.g., Gobiet et al.,~~
366 ~~2014; Smiatek et al., 2016; Steger et al., 2013) with the general effect of a decreasing snowfall~~
367 ~~frequency and fraction, thus potentially leading to a reduction in overall snowfall amounts changes.~~
368 ~~Separating the above two competing factors is one of the targets of the current study. A potential~~
369 ~~complication is that changes in daily precipitation frequency (here events > 1 mm/day) and~~
370 ~~precipitation intensity (average amount on wet days) can change in a counteracting manner (e.g.,~~
371 ~~Fischer et al., 2015; Rajczak et al., 2013), and that relative changes are not uniform across the event~~
372 ~~category (e.g. Ban et al., 2015; Fischer and Knutti, 2016).~~

373 The article is structured as follows: Section 2 describes the data used and methods employed. In
374 Sections 3 and 4 results of the bias ~~correction-adjustment~~ approach and snowfall projections for the
375 late 21st century are shown, respectively. The latter are further discussed in Section 5 while overall
376 conclusions and a brief outlook are provided in Section 6. Additional supporting figures are provided in
377 the supplementary material (prefix 'S' in Figure numbers).

378 2 Data and methods

379 2.1 Observational data

380 To estimate observation-based snowfall, two gridded data sets, one for precipitation and one for
381 temperature, derived from station observations and covering the area of Switzerland are used. Both
382 data sets are available on a daily basis with a horizontal resolution of 2 km for the entire evaluation
383 period 1971-2005 (see Sec. 2.3).

384 The gridded precipitation data set (RhiresD) represents a daily analysis based on a high-resolution
385 rain-gauge network (MeteoSwiss, 2013a) consisting of more than 400 stations which has that have a
386 balanced distribution in the horizontal but under-represents high altitudes (Frei and Schär, 1998; Isotta
387 et al., 2014; Konzelmann et al., 2007). Albeit the data set's resolution of 2 km, the effective grid
388 resolution as represented by the mean inter-station distance is about 15 - 20 km and thus comparable
389 to the nominal resolution of the available climate model data (see Sec. 2.2). The dataset has not been
390 corrected for the systematic measurement bias of rain gauges (e.g., Neff, 1977; Sevruk, 1985; Yang et
391 al., 1999).

392 The gridded near-surface air temperature (from now on simply referred to as *temperature*) data set
393 (TabsD) utilises a set of approx. 90 homogeneous long-term station series (MeteoSwiss, 2013b).
394 Despite the high quality of the underlying station series, errors might be introduced by unresolved
395 scales, an uneven spatial distribution and interpolation uncertainty (Frei, 2014). The unresolved effects
396 of land cover or local topography, for instance, probably lead to an underestimation of spatial
397 variability. ~~Another problem arises in inner Alpine valleys, where the presence of cold air pools is~~
398 ~~systematically overestimated. Also note that, while RhiresD provides daily precipitation sums~~
399 ~~aggregated from 6 UTC to 6 UTC of the following day, TabsD is a true daily temperature average from~~
400 ~~midnight UTC to midnight UTC. Due to a high temporal autocorrelation of daily mean temperature this~~
401 ~~slight inconsistency in the reference interval of the daily temperature and precipitation grids is~~
402 ~~expected to not systematically influence our analysis.~~

403 In addition to the gridded temperature and precipitation datasets and in order to validate simulated raw
404 snowfall amounts station-based observations of fresh snow sums (snow depth) at daily resolution from
405 29 stations in Switzerland with data available for at least 80% of the evaluation period 1971-2005 are
406 employed.

407 2.2 Climate model data

408 In terms of climate model data we exploit a recent ensemble of regional climate projections made
409 available by EURO-CORDEX (www.euro-cordex.net), the European branch of the World Climate
410 Research Programme's CORDEX initiative (www.cordex.org; Giorgi et al., 2009). RCM simulations for
411 the European domain were run at a resolution of approximately 50 km (EUR-44) and 12.5 km (EUR-
412 11) with both re-analysis boundary forcing (Kotlarski et al., 2014; Vautard et al., 2013) and GCM-
413 forcing (Jacob et al., 2014). ~~We here disregard the reanalysis-driven experiments and employ the. The~~
414 ~~latter include GCM-driven simulations only. These include~~ historical control simulations and future
415 projections based on RCP greenhouse gas and aerosol emission scenarios. Within the present work

416 we employ daily averaged model output of all except two¹GCM-driven EUR-11 simulations for which
417 control, RCP4.5 and RCP8.5 runs ~~are currently were~~ available in December 2016. This yields a total
418 set of 14 GCM-RCM model chains, combining five driving GCMs with seven different RCMs (Tab. 1).
419 We exclusively focus on the higher resolved EUR-11 simulations and disregard the coarser EUR-44
420 ensemble due to the apparent added value of the EUR-11 ensemble with respect to regional-scale
421 climate features in the complex topographic setting of the European Alps (e.g., Giorgi et al., 2016;
422 Torma et al., 2015).

423 It is important to note that each of the ~~sevensix~~ RCMs considered uses an individual grid cell
424 topography field. Model topographies for a given grid cell might therefore considerably differ from each
425 other, and also from the observation-based orography. Hence, it is not meaningful to compare snowfall
426 values at individual grid cells since the latter might be situated at different elevations. Therefore, most
427 analyses of the present work were carried out as a function of elevation, i.e., by averaging climatic
428 features over distinct elevation intervals.

429 **2.3 Analysis domain and periods**

430 The arc-shaped European Alps - with a West-East extent of roughly 1200 km , a total of area 190'000
431 km² and a peak elevation of 4810 m a.s.l. (Mont Blanc) - are the highest and most prominent
432 mountain range which is entirely situated in Europe. In the present work, two different analysis
433 domains are used. The evaluation of the bias ~~correction~~adjustment approach depends on the
434 observational data sets RhiresD and TabsD (see Sec. 2.1). As these cover Switzerland only, the
435 evaluation part of the study (Sec. 3) is constrained to the Swiss domain (Fig. 1, bold line). For the
436 analysis of projected changes of different snowfall indices (Sec. 4 and 5) a larger domain covering the
437 entire Alpine crest with its forelands is considered (Fig. 1, coloured region).

438 Our analysis is based on three different time intervals. The evaluation period (EVAL) 1971-2005 ~~is~~was
439 used for the calibration and validation of the bias ~~correction~~adjustment approach. Future changes of
440 snowfall indices ~~are were~~ computed by comparing a present~~-~~day control period (1981-2010, CTRL) to
441 a future scenario period at the end of the 21st century (2070-2099, SCEN). For all periods (EVAL,
442 CTRL and SCEN), the summer months June, July and August (JJA) are excluded from any statistical
443 analysis. In addition to seasonal mean snowfall conditions, i.e., averages over the nine-month period
444 from September to May, we also analyse the seasonal cycle of individual snowfall indices at monthly
445 resolution.

446 **2.4 Analysed snowfall indices and change signals**

447 A set of six different snowfall indices is considered (Tab. 2). Mean snowfall (S_{mean}) refers to the
448 (spatio-) temporally-averaged snowfall amount in mm SWE (note that from this point on we will use the
449 term "mm" as a synonym for "mm SWE" as unit of several snowfall indices). The two indices heavy
450 snowfall (S_{q99}) and maximum 1-day snowfall (S_{1d}) allow the assessment of projected changes in heavy

¹ The HadGEM2-RACMO experiments were excluded due to serious snow accumulation issues over the European Alps. Furthermore, only realization 1 of MPI-M-REMO was included in order to avoid mixing GCM-RCM sampling with pure internal climate variability sampling.

451 snowfall events and amounts. S_{1d} is derived by averaging maximum 1-day snowfall amounts over all
 452 individual months/seasons of a given time period (i.e., by averaging 30 maximum values in the case of
 453 the CTRL and SCEN period), while S_{q99} is calculated from the grid point-based 99th all-day snowfall
 454 percentile of the daily probability density function (PDF) for the entire time period considered. We use
 455 all-day percentiles as the use of wet-day percentiles leads to conditional statements that are often
 456 misleading (see the analysis in Schär et al. 2016). Note that the underlying number of days differs for
 457 seasonal (September-May) and monthly analyses. Snowfall frequency (S_{freq}) and mean snowfall
 458 intensity (S_{int}) are based on a wet-day threshold of 1 mm/day and provide additional information about
 459 the distribution and magnitude of snowfall events, while the snowfall fraction (S_{frac}) describes the ratio
 460 of solid precipitation to total precipitation. As climate models tend to suffer from too high occurrence of
 461 drizzle and as small precipitation amounts are difficult to measure, daily precipitation values smaller or
 462 equal to 0.1 mm were ~~initially~~ set to zero in both the observations and the simulations prior to the
 463 remaining analyses.

464 Projections are assessed by calculating two different types of changes between the CTRL and the
 465 SCEN period. The absolute change signal (Δ) of a particular snowfall index X (see Tab.2)

$$466 \quad \Delta X = X_{SCEN} - X_{CTRL} \quad (1)$$

467 and the relative change signal (δ) which describes the change of the snowfall index as a percentage of
 468 its CTRL period value

$$469 \quad \delta X = \left(\frac{X_{SCEN}}{X_{CTRL}} - 1 \right) \cdot 100 \quad (2)$$

470 To prevent erroneous data interpretation due to possibly ~~ye~~ large relative changes of small CTRL
 471 values, certain grid boxes were masked out before calculating and averaging the signal of change.
 472 This filtering was done by setting threshold values for individual indices and statistics (see Table 2).

473 2.5 Separating snowfall from total precipitation

474 Due to (a) the lack of a gridded observational snowfall data set and (b) the fact that not all RCM
 475 simulations available through EURO-CORDEX provide raw snowfall as an output variable, a method
 476 to separate solid from total precipitation depending on near-surface temperature conditions is
 477 developed. ~~This method also allows for a more physically-based bias correction of simulated snowfall~~
 478 ~~amounts (see Sec. 2.6). Due to the temperature dependency of snowfall occurrence, snowfall biases~~
 479 ~~of a given climate model cannot be expected to remain constant under current and future (i.e.,~~
 480 ~~warmer) climate conditions. For instance, a climate model with a given temperature bias might pass~~
 481 ~~the snow-rain temperature threshold earlier or later than reality during the general warming process.~~
 482 ~~Hence, traditional bias correction approaches based only on a comparison of observed and simulated~~
 483 ~~snowfall amounts in the historical climate would possibly fail due to a non-stationary bias structure.~~

484 The simplest approach to separate snowfall from total precipitation is to fractionate the two phases
 485 binary by applying a constant snow fractionation temperature (e.g., de Vries et al., 2014; Schmucki et
 486 al., 2015a; Zubler et al., 2014). More sophisticated methods estimate the snow fraction f_s dependence

487 on air temperature with linear or logistic relations (e.g., Kienzle, 2008; McAfee et al., 2014). In our
 488 case, the different horizontal resolutions of the observational (high resolution of 2 km) and simulated
 489 (coarser resolution of 12 km) data sets further complicate a proper comparison of the respective
 490 snowfall amounts. Thus, we explicitly analysed the snowfall amount dependency on the grid resolution
 491 and exploited possibilities for including subgrid-scale variability in snowfall separation ~~based on coarse~~
 492 ~~grid information~~. This approach is important as especially in Alpine terrain a strong subgrid-scale
 493 variability of near-surface temperatures due to orographic variability has to be expected, with
 494 corresponding effects on the subgrid-scale snowfall fraction.

495 For this preparatory analysis, which is entirely based on observational data, a reference snowfall is
 496 derived. It is based on the approximation of snowfall by application of a fixed temperature threshold to
 497 daily total precipitation amounts on the high resolution observational grid (2 km) and will be termed
 498 *Subgrid method* thereafter: First, the daily snowfall S' at each grid point of the observational data set at
 499 high resolution (2 km) is derived by applying a snow fractionation temperature $T^*=2^\circ\text{C}$. The whole
 500 daily precipitation amount P' is accounted for as snow S' (i.e., $f_s=100\%$) for days with daily mean
 501 temperature $T \leq T^*$. For days with $T > T^*$, S' is set to zero and P' is attributed as rain (i.e., $f_s=0\%$). This
 502 threshold approach with a fractionation temperature of 2°C corresponds to the one applied in previous
 503 works and results appear to be in good agreement with station-based snowfall measurements (e.g.,
 504 Zubler et al., 2014). The coarse grid (12 km) reference snowfall S_{SG} is determined by averaging the
 505 sum of separated daily high resolution S' over all n high-resolution grid points i located within a specific
 506 coarse grid point k . I.e., at each coarse grid point k

$$507 \quad S_{SG} = \frac{1}{n} \cdot \sum_{i=1}^n P'_i [T'_i \leq T^*] = \frac{1}{n} \sum_{i=1}^n S'_i \quad (3)$$

508 For comparison, the same binary fractionation method with a temperature threshold of $T^*=2^\circ\text{C}$ is
 509 directly applied on the coarse 12 km grid (*Binary method*). For this purpose, total precipitation P' and
 510 daily mean temperature T' of the high-resolution data are conservatively remapped to the coarse grid
 511 leading to P and T , respectively. Compared to the *Subgrid method*, the *Binary method* neglects any
 512 subgrid-scale variability of the snowfall fraction. As a result, the *Binary method* underestimates S_{mean}
 513 and overestimates S_{q99} for ~~most~~ elevation intervals (Fig. 2). The underestimation of S_{mean} can be
 514 explained by the fact that even for a coarse grid temperature above T^* individual high-elevation
 515 subgrid cells (at which $T \leq T^*$) can receive substantial snowfall amounts, ~~a process that is not~~
 516 ~~accounted for by the Binary method~~. As positive precipitation-elevation gradients can be assumed for
 517 most parts of the domain (larger total precipitation at high elevations; see e.g. Kotlarski et al., 2012
 518 and Kotlarski et al., 2015 for an Alpine-scale assessment) the neglect of subgrid-scale snowfall
 519 variation in the Binary method hence leads a systematic underestimation of mean snowfall compared
 520 to the Subgrid method. Furthermore, following O'Gorman (2014), heavy snowfall events are expected
 521 to occur in a narrow temperature range below the rain-snow transition. As the *Binary method* in these
 522 temperature ranges always leads to a snowfall fraction of 100%, too large S_{q99} values would result.

523 To take into account these subgrid-scale effects, a more sophisticated approach – referred to as the
 524 *Richards method* – is developed here. This method is based upon a generalised logistic regression
 525 (Richards, 1959). Here, we apply this regression to relate the surface temperature T to the snow

526 fraction f_s by accounting for the topographic subgrid-scale variability. At each coarse grid-point k , the
 527 *Richards method*-based snowfall fraction $f_{s,RI}$ for a given day is hence computed as follows:

$$528 \quad f_{s,RI}(T_k) = \frac{1}{[1 + C_k \cdot e^{D_k \cdot (T_k - T^*)}]^{C_k}} \quad (4)$$

529 with C as the point of inflexion (denoting the point with largest slope), and D the growth rate D
 530 (reflecting the mean slope). T_k is the daily mean temperature of the corresponding coarse grid box k
 531 and $T^*=2^\circ\text{C}$ the snow fractionation temperature. First, we estimate the two parameters C and D of
 532 Equation 4 for each single coarse grid point k by minimizing the least-square distance to the f_s values
 533 derived by the *Subgrid method* via the reference snowfall S_{SG} (local fit). Second, C and D are
 534 expressed as a function of the topographic standard deviation σ_h of the corresponding coarse
 535 resolution grid point only (Fig. S1; global fit). This makes it possible to define empirical functions for
 536 both C and D that can be used for all grid points k in the Alpine domain and that depend on σ_h only.

$$537 \quad \sigma_{h,k} = \sqrt{\frac{\sum_i^n (h_i - \bar{h}_k)^2}{n-1}} \quad (5)$$

$$538 \quad C_k = \frac{1}{(E - \sigma_{h,k} \cdot F)} \quad (6)$$

$$539 \quad D_k = G \cdot \sigma_{h,k}^{-H} \quad (7)$$

540 Through a minimisation of the least square differences the constant parameters in Equations 6 and 7
 541 are calibrated over the domain of Switzerland and using daily data from the period September to May
 542 1971-2005 leading to values of $E=1.148336$, $F=0.000966 \text{ m}^{-1}$, $G=143.84113 \text{ }^\circ\text{C}^{-1}$ and $H=0.8769335$.
 543 Note that σ_h is sensitive to the resolution of the two grids to be compared (cf. Eq. 5). It is a measure for
 544 the uniformity of the underlying topography and has been computed based on the high-resolution
 545 [GTOPO30 digital elevation model \(https://lta.cr.usgs.gov/GTOPO30\)](https://lta.cr.usgs.gov/GTOPO30) aggregated to a regular grid of
 546 [1.25 arc seconds \(about 2 km\) which reflects the spatial resolution of the observed temperature and](#)
 547 [precipitation grids \(cf. Section 2.1\)](#). Small values of σ_h indicate a low subgrid-scale topographic
 548 variability, such as in the Swiss low-lands, while high values result from non-uniform elevation
 549 distributions, such as in areas of inner Alpine valleys. σ_h as derived from GTOPO30 might be different
 550 from the subgrid-scale topographic variance employed by the climate models themselves, which is
 551 however not relevant here as only grid cell-averaged model output is analysed and as we considere σ_h
 552 as a proper estimate of subgrid-scale variability.

553 Figure S1 (panel c) provides an example of the relation between daily mean temperature and daily
 554 snow fraction f_s for grid cells with topographical standard deviations of 50 m and 500 m, respectively.
 555 The snowfall amount S_{RI} for a particular day and a particular coarse grid box is finally obtained by
 556 multiplying the corresponding $f_{s,RI}$ and P values. A comparison with the *Subgrid method* yields very
 557 similar results. For both indices S_{mean} and S_{q99} , mean ratios across all elevation intervals are close to 1
 558 (Fig. 2). At single grid points, maximum deviations are not larger than 1 ± 0.1 . Note that for this
 559 comparison calibration and validation period are identical (EVAL period). Based on this analysis, it has
 560 been decided to separate snowfall according to the *Richards method* throughout this work in both the

561 observations and in the RCMs. The observation-based snowfall estimate obtained by applying the
562 *Richards method* to the observational temperature and precipitation grids after spatial aggregation to
563 the 0.11° RCM resolution will serve as reference for the RCM bias ~~correction~~adjustment and will be
564 termed *reference* hereafter. One needs to bear in mind that the parameters *C* and *D* of the Richards
565 method were fitted for the Swiss domain only and were later on applied to the entire Alpine domain (cf.
566 Fig. 1).

567 **2.6 Bias ~~correction~~adjustment approach**

568 Previous work has revealed partly substantial temperature and precipitation biases of the EURO-
569 CORDEX RCMs over the Alps (e.g. Kotlarski et al., 2014; Smiatek et al., 2016), and one has to expect
570 that the separated snowfall amounts are biased too. This would especially hamper the interpretation of
571 absolute climate change signals of the considered snow indices. We therefore explore possibilities to
572 bias-~~adjust~~correct the simulated snowfall amounts and to directly integrate this bias ~~correction~~
573 adjustment into the snowfall separation framework of Section 2.5. Note that we deliberately employ the
574 term *bias adjustment* as opposed to *bias correction* to make clear that only certain aspects of the
575 snowfall climate are adjusted and that the resulting dataset might be subject to remaining
576 inaccuracies.

577 ~~We compare results with and without employment of the bias correction procedure outlined below.~~ A
578 simple two-step approach that separately accounts for precipitation and temperature biases and their
579 respective influence on snowfall is chosen. The separate consideration of temperature and
580 precipitation biases allows for a more physically-based bias adjustment of snowfall amounts: Due to
581 the temperature dependency of snowfall occurrence, snowfall biases of a given climate model cannot
582 be expected to remain constant under current and future (i.e., warmer) climate conditions. For
583 instance, a climate model with a given temperature bias might pass the snow-rain temperature
584 threshold earlier or later than reality during the general warming process. Hence, traditional bias
585 adjustment approaches based only on a comparison of observed and simulated snowfall amounts in
586 the historical climate would possibly fail due to a non-stationary bias structure. The bias ~~correction~~
587 adjustment is calibrated in the EVAL period for each individual GCM-RCM chain and over the region of
588 Switzerland, and is then applied to both the CTRL and SCEN period of each chain and for the entire
589 Alpine domain. To be consistent in terms of horizontal grid spacing, the observational data sets
590 RhiresD and TabsD (see Sec. 2.1) are conservatively regridded to the RCM resolution beforehand.

591 In a first step, total simulated precipitation was adjusted by introducing an elevation-dependent
592 ~~correction~~adjustment factor which ~~corrects for~~adjusts precipitation biases regardless of temperature.
593 For this purpose, mean precipitation ratios (RCM simulation divided by observational analysis) for 250
594 m elevation intervals were calculated (Fig. S2). An almost linear relationship of these ratios with
595 elevation was found. Thus, a linear regression between the intervals from 250 m a.s.l. to 2750 m a.s.l.
596 was used for each model chain separately to estimate a robust ~~correction~~adjustment factor. As the
597 number of both RCM grid points and measurement stations at very high elevations (>2750 m a.s.l.) is
598 small (see Sec. 2.1) and biases are subject to a considerable sampling uncertainty, these elevations
599 were not considered in the regression. Overall the fits are surprisingly precise except for the altitude

600 bins above 2000 m (Fig. S2). The precipitation adjustment factors (P_{AF}) for a given elevation were then
601 obtained as the inverse of the fitted precipitation ratios. Multiplying simulated precipitation P with P_{AF}
602 for the respective model chain and elevation results in the ~~corrected-adjusted~~ precipitation:

$$603 \quad P_{\text{corr-adj}} = P \cdot P_{AF} \quad (8)$$

604 For a given GCM-RCM chain and for each elevation interval, the spatially and temporally averaged
605 corrected total precipitation $P_{\text{corr-adj}}$ approximately corresponds to the observation-based estimate in
606 the EVAL period.

607 In the second step of the bias ~~adjustment~~correction procedure, temperature biases are accounted
608 for. For this purpose the initial snow fractionation temperature $T^*=2^\circ\text{C}$ of the Richards separation
609 method (see Sec 2.5) is shifted to the value T_a^* for which the spatially (Swiss domain) and temporally
610 (September to May) averaged simulated snowfall amounts for elevations below 2750 m a.s.l. match
611 the respective observation-based reference (see above). Compared to the adjustment of total
612 precipitation, T_a^* is chosen independent of elevation, but separately for each GCM-RCM chain, in
613 order to avoid overparameterization and to not over-interpret the elevation dependency of mean
614 snowfall in the snowfall reference grid. After this second step of the bias ~~adjustment~~correction, the
615 spatially ~~(Swiss domain)~~ and temporally ~~(September to May)~~ averaged simulated snowfall amounts
616 below 2750 m a.s.l. by definition match the reference by definition. Hence, the employed simple bias
617 ~~adjustment~~ correction procedure ~~corrects-adjusts~~ domain-mean snowfall biases averaged over the
618 entire season from September to May. It does, however, not correct for biases in the spatial snowfall
619 pattern, in the seasonal cycle, or in the temporal distribution of daily values. Note that, as the
620 underlying high-resolution data sets are available over Switzerland only, the calibration of the bias
621 ~~correction~~ adjustment methodology is correspondingly restricted, but the ~~correction~~ adjustment is then
622 applied to the whole Alpine domain. This approach is justified as elevation-dependent mean winter
623 precipitation and temperature biases of the RCMs employed – assessed by comparison against the
624 coarser-resolved EOBS reference dataset (Haylock et al., 2008) - are very similar ~~for over~~ Switzerland
625 and ~~for over~~ the entire Alpine analysis domain (Figs. S3 and S4).

626 **3 Evaluation**

627 **3.1 RCM raw snowfall**

628 We first carry out an illustrative comparison of RCM raw snowfall amounts (for those simulations only
629 that directly provide snowfall flux) against station observations of snowfall, in order to determine
630 whether the simulated RCM snowfall climate contains valid information despite systematic biases. To
631 this end, simulated raw snowfall amounts of nine EURO-CORDEX simulations (see Tab. 1) averaged
632 over 250 m-elevation intervals and over in the range 950 – 1650 m a.s.l. are compared against
633 observations ~~derived from of~~ measured fresh snow sums from 29 MeteoSwiss stations (see Section
634 2.1), with data available for at least 80% of the EVAL period. For this purpose a mean snow density of
635 100 kg/m^3 for the conversion from measured snow height-depth to water equivalent is assumed. Note
636 that this simple validation is subject to considerable uncertainties as it does not explicitly correct for the

637 scale and elevation gap between grid-cell based RCM output and single-site observations. Especially
638 in complex terrain and for exposed sites, point measurements of snow depth might be non-
639 representative for larger-scale conditions (e.g., Grünewald and Lehning, 2015). Also, the conversion
640 from snow depth to snow water equivalent is of approximate nature only, and fresh snow sums might
641 furthermore misrepresent true snowfall in case that snow melt or snow drift occurs between two snow
642 depth readings.

643 At low elevations simulated mean September-May raw snowfall sums match the observations well
644 while differences are larger aloft (Fig. 3a). The positive bias at high elevations might arise from the fact
645 that (the very few) observations were made at ~~a~~ specific locations while simulated grid point values of
646 the corresponding elevation interval might be located in different areas of Switzerland. It might also be
647 explained by positive RCM precipitation and negative RCM temperature biases at high elevations of
648 the Alps (e.g., Kotlarski et al., 2015). At lower elevations, the station network is geographically more
649 balanced and the observations are probably more representative of the respective elevation interval.
650 Despite a clear positive snowfall bias in mid-winter, the RCMs are generally able to reproduce the
651 mean seasonal cycle of snowfall for elevations between 950 m a.s.l. - 1650 m a.s.l. (Fig. 3b). The fact
652 that the major patterns of both the snowfall-elevation relationship and the mean seasonal snowfall
653 cycle are basically well represented indicates the general and physically consistent applicability of
654 RCM output to assess future changes in mean and heavy Alpine snowfall. However, substantial
655 biases in snowfall amounts are apparent and a bias ~~correction~~ adjustment of simulated snowfall
656 seems to be required prior to the analysis of climate change signals of individual snowfall indices.

657 **3.2 Evaluation of the reference snowfall**

658 The snowfall separation employing the Richards method (Section 2.5) and, as a consequence, also
659 the bias adjustment (Section 2.6) make use of the 2 km reference snowfall grid derived by employing
660 the Subgrid method on the observed temperature and precipitation grids. Hence, the final results of
661 this study could to some extent be influenced by inaccuracies and uncertainties of the reference
662 snowfall grid itself. In order to assess the quality of the latter and in absence of a further observation-
663 based reference we here present an approximate evaluation.

664 First, the reference snowfall grid is evaluated against fresh snow sums at the 29 Swiss stations that
665 were also used for evaluating RCM raw snowfall. Note the limitations of such a comparison as outlined
666 in Chapter 3.1. The comparison of black and red markers and lines in Figure 3 indicates a good
667 agreement of mean snowfall at individual elevation intervals (left panel) as well for the mean annual
668 cycle of snowfall at medium elevations (right panel). The reference snowfall grid is obviously a good
669 approximation of site-scale fresh snow sums. Note that similarly to the RCM raw snowfall evaluation,
670 all 2 km reference snowfall grid cells in the respective elevation interval are considered. The good
671 agreement, however, still holds if only those 2 km grid cells covering the 29 site locations are
672 considered (not shown here).

673 Second, both the 2 km reference snowfall grid and the 0.11° reference snowfall grid obtained by
674 employing the Richards method to aggregated temperature and precipitation values (see Section 2.5)
675 are compared against the gridded HISTALP dataset of solid precipitation (Chimani et al., 2011). The

676 latter is provided at a monthly resolution on a 5' grid covering the Greater Alpine Region. It is based on
677 monthly snowfall fraction estimates that are used to scale a gridded dataset of total precipitation. The
678 comparison of the three datasets for the region of Switzerland (for which the 2 km reference snowfall
679 is available) in the EVAL period 1971-2005 yields an approximate agreement of both the magnitude of
680 mean winter snowfall and its spatial pattern. The three data sets differ with respect to their spatial
681 resolution but all show a clear dependency of snowfall on topography and mean September-May
682 snowfall sums above 1000 mm over most parts of the Alpine ridge. Climatologically warm and dry
683 valleys, on the other hand, are represented by minor snowfall amounts of less than 400 m only.

684 As mentioned before these evaluations of the reference snowfall grid are subject to uncertainties and,
685 furthermore, they only cover mean snowfall amounts. However, they provide basic confidence in the
686 applicability of the reference snowfall grid for the purposes of snowfall separation and bias adjustment
687 in the frame of the present study.

689 **3.32 Calibration of bias ~~correction~~-adjustment**

690 The analysis of total precipitation ratios (RCM simulations with respect to observations) for the EVAL
691 period, which are computed to carry out the first step of the bias ~~correction~~-adjustment procedure,
692 reveals substantial elevation dependencies. All simulations tend to overestimate total precipitation at
693 high elevations (Fig. S24). This fact might ultimately be connected to an overestimation of surface
694 snow amount in several EURO-CORDEX RCMs as reported by Terzago et al. (2017). As the
695 precipitation ratio between simulations and observations depends approximately linearly ~~depends~~ on
696 elevation, the calculation of P_{AF} via a linear regression of the ratios against elevation (see Sec. 2.6)
697 seems reasonable. By taking the inverse of this linear relation, P_{AF} for every model and elevation can
698 be derived. For the CCLM and RACMO simulations, these correction factors do not vary much with
699 height, while P_{AF} for MPI-ESM - REMO and EC-EARTH - HIRHAM is much larger than 1 in low lying
700 areas, indicating a substantial underestimation of observed precipitation sums (Fig. 4a). However, for
701 most elevations and simulations, P_{AF} is generally smaller than 1, i.e., total precipitation is
702 overestimated by the models. Similar model biases in the winter and spring seasons have already
703 been reported in previous works (e.g., Rajczak et al., in prep.; Smiatek et al., 2016). Especially at high
704 elevations, these apparent positive precipitation biases could be related to observational undercatch,
705 i.e., an underestimation of true precipitation sums by the observational analysis. Frei et al. (2003)
706 estimated seasonal Alpine precipitation undercatch for three elevation intervals. Results show that
707 measurement biases are largest in winter and increase with altitude. However, a potential undercatch
708 (with a maximum of around 40% at high elevations in winter; Frei et al., 2003) can only partly explain
709 the partly substantial overestimation of precipitation found in the present work.

710 After applying P_{AF} to the daily precipitation fields, a snowfall fractionation at the initial T^* of 2 °C (see
711 Eq. (4)) would lead to a snowfall excess in all 14 simulations as models typically experience a cold
712 winter temperature bias. To match the observation-based and spatio-temporally averaged reference
713 snowfall below 2750 m a.s.l., T^* for all models needs to be decreased during the second step of the
714 bias ~~correction~~-adjustment (Fig 4b). The adjusted T_a^* values indicate a clear positive relation with the

715 mean temperature bias in the EVAL period. This feature is expected since the stronger a particular
716 model's cold bias the stronger the required adjustment of the snow fractionation temperature T^*
717 towards lower values in order to avoid a positive snowfall bias. Various reasons for the scatter around
718 a simple linear relation in Figure 4b can be thought of. These include remaining spatial inaccuracies of
719 the corrected precipitation grid, elevation-dependent temperature biases and misrepresented
720 temperature-precipitation relationships at daily scale. Note that precipitation and temperature biases
721 heavily depend on the GCM-RCM chain and seem to be rather independent from each other. While
722 EC-EARTH – RACMO, for instance, shows one of the best performances in terms of total
723 precipitation, its temperature bias of close to -5 °C is the largest deviation in our set of simulations.
724 Concerning the partly substantial temperature biases of the EURO-CORDEX models shown in Figure
725 4 b, their magnitude largely agrees with Kotlarski et al. (2014; in reanalysis-driven simulations) and
726 Smiatek et al. (2016).

727 **3.43 Evaluation of snowfall indices**

728 We next assess the performance of the bias correction-adjustment procedure by comparing snowfall
729 indices derived from separated and bias-corrected-adjusted RCM snowfall amounts against the
730 observation-based reference. The period for which this comparison is carried out is EVAL, i.e., it is
731 identical to the calibration period of the bias correction-adjustment. We hence do not intend a classical
732 cross validation exercise with separate calibration and validation periods, but try to answer the
733 following two questions: (a) Which aspects of the Alpine snowfall climate are corrected-for-adjusted,
734 and (b) for which aspects do biases remain even after application of the bias correction-adjustment
735 procedure.

736 Figure 5 shows the evaluation results of the six snowfall indices based on the separated and not bias-
737 corrected-adjusted simulated snowfall ($RCM_{sep+nb_{ae}}$), and the separated and bias-corrected-adjusted
738 simulated snowfall ($RCM_{sep+b_{ae}}$). In the first case the snowfall separation of raw precipitation is
739 performed with $T^*=2^{\circ}C$, while in the second case precipitation is corrected-adjusted and the separation
740 is performed with a bias-adjusted temperature T^*_a . The first column represents the mean September
741 to May statistics, while columns 2-4 depict the seasonal cycle at monthly resolution for three distinct
742 elevation intervals.

743 The analysis of S_{mean} confirms that $RCM_{sep+b_{ae}}$ is able to reproduce the observation-based reference in
744 the domain mean as well as in most individual elevation intervals. The domain-mean agreement is a
745 direct consequence of the design of the bias correction-adjustment procedure (see above).
746 $RCM_{sep+nb_{ae}}$, on the other hand, consistently overestimates S_{mean} by up to a factor of 2.5 as a
747 consequence of positive precipitation and negative temperature biases (cf. Fig. 4). Also the seasonal
748 cycle of S_{mean} for $RCM_{sep+b_{ae}}$ yields a satisfying performance across all three elevation intervals, while
749 $RCM_{sep+nb_{ae}}$ tends to produce too much snowfall over all months and reveals an increasing model
750 spread with elevation.

751 For the full domain and elevations around 1000 m, the observation-based reference indicates a mean
752 S_{freq} of 20% between September and May. Up to 1000 m a.s.l. $RCM_{sep+b_{ae}}$ reflects the increase of this

753 index with elevation adequately. However, towards higher elevations the approximately constant S_{freq}
754 of 30% in the reference is not captured by the simulation-derived snowfall. Notably during wintertime,
755 both $\text{RCM}_{\text{sep+b}_{\text{ae}}}$ and $\text{RCM}_{\text{sep+nb}_{\text{ae}}}$ produce too many snowfall days, i.e., overestimate snowfall
756 frequency. This feature is related to the fact that climate models typically tend to overestimate the wet
757 day frequency over the Alps especially in wintertime (Rajczak et al., 2013) and that the bias ~~correction~~
758 adjustment procedure employed does not explicitly correct for potential biases in precipitation
759 frequency. Due to the link between mean snowfall on one side and snowfall frequency and mean
760 intensity on the other side, opposite results are obtained for the mean snowfall intensity S_{int} .
761 $\text{RCM}_{\text{sep+b}_{\text{ae}}}$ largely underestimates mean intensities during snowfall days while $\text{RCM}_{\text{sep+nb}_{\text{ae}}}$ typically
762 better reflects the reference. Nevertheless, deviations during winter months at mid-elevations are not
763 negligible. Mean September-May S_{frac} in the reference exponentially increases with elevation. This
764 behaviour is reproduced by both $\text{RCM}_{\text{sep+b}_{\text{ae}}}$ and $\text{RCM}_{\text{sep+nb}_{\text{ae}}}$. Notwithstanding, $\text{RCM}_{\text{sep+b}_{\text{ae}}}$ results are
765 more accurate compared to $\text{RCM}_{\text{sep+nb}_{\text{ae}}}$, which turns out to be biased towards too large snowfall
766 fractions.

767 For the two heavy snowfall indices S_{q99} and $S_{1\text{d}}$, $\text{RCM}_{\text{sep+nb}_{\text{ae}}}$ appears to typically match the reference
768 better than $\text{RCM}_{\text{sep+b}_{\text{ae}}}$. Especially at high elevations, $\text{RCM}_{\text{sep+b}_{\text{ae}}}$ produces too low snowfall amounts.
769 This again ~~highlights-illustrates~~ the fact that the bias ~~adjustment correction~~ procedure is designed to
770 ~~correct-adjust for~~ biases in mean snowfall, but does not necessarily improve further aspects of the
771 simulated snowfall climate.

772 The spatial patterns of S_{mean} for the 14 $\text{RCM}_{\text{sep+b}_{\text{ae}}}$ simulations from September to May are presented
773 in Figure 6. The observational-based reference (lower right panel) reveals a snowfall distribution with
774 highest values along the Alpine main ridge, whereas the Swiss plateau, Southern Ticino and main
775 valleys such as the Rhône and Rhine valley experience less snowfall. Almost all bias-~~corrected~~
776 adjusted models are able to represent the overall picture with snow-poor lowlands and snow-rich
777 Alpine regions. Nevertheless substantial differences to the observations concerning the spatial
778 snowfall pattern can arise. EC-EARTH - HIRHAM, for example, is subject to a "pixelated" structure.
779 This could be the result of frequent grid-cell storms connected to parameterisations struggling with
780 complex topographies. Such inaccuracies in the spatial pattern are not corrected for by our simple bias
781 ~~correction-adjustment~~ approach ~~which that~~ only targets domain-mean snowfall amounts at elevations
782 below 2750 m a.s.l. and that does not considerably modify the simulated spatial snowfall patterns..
783 Note that these patterns are obviously strongly determined by the RCM itself and only slightly depend
784 on the driving GCM (see, for instance, the good agreement among the CCLM and the RCA
785 simulations).

786 In summary, after applying the bias ~~adjustment correction~~ to the simulations most snowfall indices are
787 fairly well represented at elevations below 1000 m a.s.l.. With increasing altitude and smaller sample
788 sizes in terms of number of grid cells, reference and $\text{RCM}_{\text{sep+b}_{\text{ae}}}$ diverge. This might be caused by the
789 remaining simulated overestimation of S_{freq} and an underestimation of S_{int} . While the bias adjustment
790 ~~correction~~ approach leads to a reduction of S_{int} due to the total precipitation adjustment, S_{freq} is only
791 slightly modified by this correction and by the adjustment of T^* . Nevertheless, these two parameters

792 strongly influence other snowfall indices. The counteracting effects of overestimated S_{freq} and
793 underestimated S_{int} result in appropriate amounts of S_{mean} whereas discrepancies for S_{q99} and S_{1d} are
794 mainly driven by the underestimation of S_{int} .

795 **4 Snowfall projections for the late 21st century**

796 For the study of climate change signals, the analysis domain is extended to the entire Alps (see Sec.
797 2.3). Due to the identified difficulties of bias-~~correcting~~-~~adjusting~~ certain snowfall indices (see Sec
798 3.43), emphasis is laid upon relative signals of change (see Eq. 2). This type of change can be
799 expected to be less dependent on the remaining inaccuracies after the ~~correction~~adjustment. If not
800 stated otherwise, all results in this Section are based on the RCM_{sep+base} data, i.e., on separated and
801 bias-~~corrected~~-~~adjusted~~ RCM snowfall, and on the RCP8.5 emission scenario.

802 Projections for seasonal S_{mean} show a considerable decrease over the entire Alpine domain (Fig. 7).
803 Most RCMs project largest percentage losses of more than 80% across the Alpine forelands and
804 especially in its topographic depressions such as the Po and Rhone vValleys ~~or Western France~~. Over
805 the Alpine ridge, reductions are smaller but still mostly negative. Elevated regions between
806 Southeastern Switzerland, Northern Italy and Austria seem to be least affected by the overall snowfall
807 reduction. Some of the simulations (e.g., CNRM-RCA, MPI-ESM-RCA or MPI-ESM-REMO) project
808 only minor changes in these regions. Experiments employing the same RCM but different driving
809 GCMs (e.g. the four simulations of RCA), but also experiments employing the same GCM but different
810 RCMs (e.g. the four simulations driven by EC-EARTH, though different realizations) can significantly
811 disagree in regional-scale change patterns and especially in the general magnitude of change. This
812 highlights a strong influence of both the driving GCMs and the RCMs themselves on snowfall changes,
813 representing effects of ~~large-scale~~ circulation and meso-scale response, respectively.

814 A more detailed analysis is provided in Fig. 8 ~~that~~-which addresses the vertical and seasonal
815 distribution of snowfall changes. It reveals that relative (seasonal mean) changes of S_{mean} appear to be
816 strongly dependent on elevation (Fig.8, top left panel). The multi-~~model~~ mean change ranges from -
817 80% at low elevations to -10% above 3000 m a.s.l.. Largest differences between neighbouring
818 elevation intervals are obtained from 750 m a.s.l. to 1500 m a.s.l.. Over the entire Alps, the results
819 show a reduction of S_{mean} by -35% to -55% with a multi-~~model~~ mean of -45%. The multi-~~model~~ spread
820 appears to be rather independent of elevation and is comparably small, confirming that, overall, the
821 spatial distributions of the change patterns are similar across all model chains (cf. Fig. 7). All
822 simulations point to decreases over the entire nine-month period September to May for the two
823 elevation intervals <1000 m a.s.l. and 1000 to 2000 m a.s.l.. Above 2000 m a.s.l., individual
824 simulations show an increase of S_{mean} by up to 20% in mid-winter which ~~forces the leads to a slightly~~
825 positive change in multi-~~model~~ mean ~~change to be slightly positive~~ in January and February.

826 Decreases of S_{freq} are very similar to change-s_{in} mean snowfall. Mean September-May changes are
827 largest below 1000 m a.s.l., while differences among elevation intervals become smaller ~~in the upper~~
828 part at higher elevations. In-between is a transition zone with rather strong changes with elevation,
829 which approximately corresponds to the mean elevation of the September-May zero-degree line in

830 | [today's climate \(e.g., Ceppi et al., 2012; MeteoSchweiz, 2016\)](#). Individual simulations with large
831 reductions in S_{mean} , such as the RCA experiments, also project strongest declines in S_{freq} . In contrast,
832 the mean snowfall intensity S_{int} is subject to smallest percentage variations in our set of snowfall
833 indices. Strong percentage changes for some models in September are due to the small sample size
834 (only few grid points considered) and the low snowfall amounts in this month. Apart from mid
835 elevations with decreases of roughly -10%, mean intensities from September to May are projected to
836 remain almost unchanged by the end of the century. For both seasonal and monthly changes, model
837 | agreement is best for high elevations while the multi-model spread is largest for lowlands. Large model
838 spread at low elevations might be caused by the small number of grid points used for averaging over
839 the respective elevation interval, especially in autumn and spring.

840 Similar results are obtained for the heavy snowfall indices S_{q99} and S_{1d} . While percentage decreases
841 at lowermost elevations are even larger than for S_{mean} , losses at high elevations are less pronounced,
842 resulting in similar domain-mean change signals for heavy and mean snowfall. Substantial differences
843 between monthly δS_{q99} and δS_{1d} appear at elevations below 1000 m a.s.l.. Here, percentage losses of
844 S_{q99} are typically slightly more pronounced. Above 2000 m a.s.l. both indices appear to remain almost
845 | constant between January and March with change signals close to zero. The multi-model mean
846 changes even hint to slight increases of both indices. Concerning changes in the snowfall fraction, i.e.,
847 in the relative contribution of snowfall to total precipitation, our results indicate that current seasonal
848 and domain mean S_{frac} might drop by about -50% (Fig. 8, lowermost row). Below 1000 m a.s.l., the
849 | strength of the signal is almost independent of the month, and multi-model average changes of the
850 snow fraction of about -80% are obtained. At higher elevations changes during mid-winter are less
851 pronounced compared to autumn and spring but still negative.

852 **5 Discussion**

853 **5.1 Effect of temperature, snowfall frequency and intensity on snowfall changes**

854 The results in Section 4 indicate substantial changes of snowfall indices over the Alps in regional
855 climate projections. With complementary analyses presented in Figures 9 and 10 we shed more light
856 on the responsible mechanisms, especially concerning projected changes in mean and heavy
857 snowfall. For this purpose Figures 9a-b,e-f show the relationship of both mean and heavy snowfall
858 amounts in the CTRL period and their respective percentage changes with the climatological CTRL
859 temperature of the respective (climatological) month, elevation interval and GCM-RCM chain. For
860 absolute amounts (S_{mean} , S_{q99} ; Fig. 9a,e) a clear negative relation is found, i.e., the higher the CTRL
861 temperature the lower the snowfall amounts. For S_{mean} the relation levels off at mean temperatures
862 higher than about 6°C with mean snowfall amounts close to zero. For temperatures below about -6°C
863 a considerable spread in snowfall amounts is obtained, i.e., mean temperature does not seem to be
864 the controlling factor here. Relative changes of both quantities (Fig. 9b,f), however, are strongly
865 controlled by the CTRL period's temperature level with losses close to 100% for warm climatic settings
866 and partly increasing snowfall amounts for colder climates. This dependency of relative snowfall
867 changes on CTRL temperature is in line with previous works addressing future snowfall changes on

868 both hemispheric and regional scales (de Vries et al., 2014; Krasting et al., 2013; Räisänen, 2016).
869 The spread of changes within a given CTRL temperature bin can presumably be explained by the
870 respective warming magnitudes that differ between elevations, months and GCM-RCM chains. About
871 half of this spread can be attributed to the month and the elevation alone (compare the spread of the
872 | black markers to the one of the red markers which indicate multi-model averages).

873 For most months and elevation intervals, percentage reductions in S_{mean} and S_{q99} reveal an almost
874 linear relationship with δS_{freq} (Fig. 9c, g). The decrease of S_{freq} with future warming can be explained
875 by a shift of the temperature probability distribution towards higher temperatures, leading to fewer
876 days below the freezing level (Fig. 10, top row). Across the three elevation intervals <1000 m a.s.l.,
877 | 1000-2000 m a.s.l. and > 2000 m a.s.l., relative changes in the number of days with temperatures
878 below the freezing level ($T \leq 0^\circ\text{C}$) are in the order of -65%, -40% and -20%, respectively (not shown).
879 This approximately corresponds to the simulated decrease of S_{freq} (cf. Fig 8), which in turn, is of a
880 similar magnitude as found in previous works addressing future snowfall changes in the Alps
881 (Schmucki et al., 2015b; Zubler et al., 2014). Due to the general shift of the temperature distribution
882 and the “loss” of very cold days (Fig. 10, top row) future snowfall furthermore occurs in a narrower
883 temperature range (Fig. 10, second row).

884 Contrasting this general pattern of frequency-driven decreases of both mean and heavy snowfall, no
885 changes or even slight increases of S_{mean} , S_{q99} and S_{1d} at high elevations are expected in mid-winter
886 (see Fig. 8). This can to some part be explained by the general increase of total winter precipitation
887 (Rajczak et al., in prep; Smiatek et al., 2016) that obviously offsets the warming effect in high-elevation
888 regions where a substantial fraction of the future temperature PDF is still located below the rain-snow
889 transition (Fig. 10, top row). This process has also been identified in previous works to be, at last
890 partly, responsible for future snowfall increases (de Vries et al., 2014; Krasting et al., 2013; Räisänen,
891 2016). Furthermore, the magnitude of the increases of both mean and heavy snowfall is obviously
892 driven by positive changes of S_{int} , while S_{freq} remains constant (Fig. 9c,g). An almost linear relationship
893 between positive changes of S_{int} and positive changes of S_{mean} and S_{q99} is obtained (Fig. 9d,h; upper
894 right quadrants). Nevertheless, the high-elevation mid-winter growth in S_{mean} is smaller than the
895 identified increases of mean winter total precipitation. This can be explained by the persistent
896 decrease of S_{frac} during the cold season (see Fig. 8, lowermost row).

897 For elevation intervals with simulated monthly temperatures between -6°C and 0°C in the CTRL
898 period, S_{mean} appears to decrease stronger than S_{q99} (cf. Fig. 9b,f). O’Gorman (2014) found a very
899 similar behaviour when analysing mean and extreme snowfall projections over the Northern
900 Hemisphere within a set of GCMs. This finding is related to the fact that future snowfall decreases are
901 mainly governed by a decrease of snowfall frequency while snowfall increases in high-elevated
902 regions in mid-winter seem to be caused by increases of snowfall intensity. It can obviously be
903 explained by the insensitivity of the temperature interval at which extreme snowfall occurs to climate
904 warming and by the shape of the temperature – snowfall intensity distribution itself (Fig. 10, third row).
905 The likely reason behind positive changes of S_{int} at high-elevated and cold regions is the higher water
906 holding capacity of the atmosphere in a warmer climate. According to the Clausius-Clapeyron relation,

907 saturation vapour pressure increases by about 7% per degree warming (Held and Soden, 2006).
908 Previous studies have shown that simulated changes of heavy and extreme precipitation (though not
909 necessarily targeting the daily temporal scale and moderate extremes as in our case) are consistent
910 with this theory (e.g., Allen and Ingram, 2002; Ban et al., 2015). In terms of snowfall, we find the
911 Clausius-Clapeyron relation to be applicable for negative temperatures up to approximately -5°C as
912 well (Fig. 10, third row, dashed lines). Inconsistencies for temperatures between -5°C and 0°C are due
913 to a snow fraction $sf < 100\%$ for corresponding precipitation events.

914 For further clarification, Figure 11 schematically illustrates the governing processes behind the
915 changes of mean and heavy snowfall that differ between climatologically warm (decreasing snowfall)
916 and climatologically cold climates (increasing snowfall). As shown in Figure 10 (third row), the mean
917 S_{int} distribution is rather independent on future warming and similar temperatures are associated with
918 similar mean snowfall intensities. In particular, heaviest snowfall is expected to occur slightly below the
919 freezing level in both the CTRL and the SCEN period (Fig. 11a). How often do such conditions prevail
920 in the two periods? In a warm current climate, i.e., at low elevations or in the transition seasons, heavy
921 snowfall only rarely occurs as the temperature interval for highest snowfall intensity is already situated
922 in the left tail of the CTRL period's temperature distribution (Fig. 11b). With future warming, i.e., with a
923 shift of the temperature distribution to the right, the probability for days to occur in the heavy snowfall
924 temperature interval (dark grey shading) decreases stronger than the probability of days to occur in
925 the overall snowfall regime (light grey shading). This results in (1) a general decrease of snowfall
926 frequency, (2) a general decrease of mean snowfall intensity and (3) a general and similar decrease of
927 both mean and heavy snowfall amounts. In contrast, at cold and high-elevated sites CTRL period
928 temperatures are often too low to trigger heavy snowfall since a substantial fraction of the temperature
929 PDF is located to the left of the heavy snowfall temperature interval (Fig. 11 c). The shifted distribution
930 in a warmer SCEN climate, however, peaks within the temperature interval that favours heavy
931 snowfall. This leads to a probability increase for days to occur in the heavy snowfall temperature range
932 despite the general reduction in S_{req} (lower overall probability of days to occur in the entire snowfall
933 regime, light grey). As a consequence, mean S_{int} tends to increase and the reduction of heavy
934 snowfall amounts is less pronounced (or even of opposing sign) than the reduction in mean snowfall.
935 For individual (climatologically cold) regions and seasons, the increase of mean S_{int} might even
936 compensate the S_{req} decrease, resulting in an increase of both mean and heavy snowfall amounts.
937 Note that in a strict sense these explanations only hold in the case that the probability of snowfall to
938 occur at a given temperature does not change considerably between the CTRL and the SCEN period.
939 This behaviour is approximately given-found (Fig. 10, bottom row), which presumably indicates only
940 minor contributions of large scale circulation changes and associated humidity changes on both the
941 temperature - snowfall frequency and the temperature - snowfall intensity relation.

942 **5.2 Emission scenario uncertainty**

943 The projections presented in the previous sections are based on the RCP8.5 emission scenario, but
944 will depend on the specific emission-scenario considered. To assess this type of uncertainty we here
945 compare the RCM_{sep+b_{ae}} simulations for the previously shown RCP8.5 emission scenario against those
946 assuming the more moderate RCP4.5 scenario. As a general picture, the weaker RCP4.5 scenario is

947 associated with less pronounced changes of snowfall indices (Fig. 12). Differences in mean seasonal
948 δS_{mean} between the two emission scenarios are most pronounced below 1000 m a.s.l. where
949 percentage changes for RCP4.5 are about one third smaller than for RCP8.5. At higher elevations,
950 multi-model mean changes better agree and the multi-model ranges for the two emission scenarios
951 start overlapping, i.e., individual RCP4.5 experiments can be located in the RCP8.5 multi-model range
952 and vice versa. Over the entire Alpine domain, about -25% of current snowfall is expected to be lost
953 under the moderate RCP4.5 emission scenario while a reduction of approximately -45% is projected
954 for RCP8.5. For seasonal cycles, the difference of δS_{mean} between RCP4.5 and RCP8.5 is similar for
955 most months and slightly decreases with altitude. Above 2000 m a.s.l., the simulated increase of S_{mean}
956 appears to be independent of the chosen RCP in January and February, while negative changes
957 before and after mid-winter are more pronounced for RCP8.5. Alpine domain mean δS_{q99} almost
958 doubles under the assumption of stronger GHG emissions. This is mainly due to differences at low
959 elevations whereas above 2000 m a.s.l. δS_{q99} does not seem to be strongly affected by the choice of
960 the emission scenario. Differences in monthly mean changes are in close analogy to δS_{mean} . Higher
961 emissions lead to a further negative shift in δS_{q99} . Up to mid-elevations differences are rather
962 independent of the season. However, at highest elevations and from January to March, differences
963 between RCP4.5 and RCP8.5 are very small.

964 Despite the close agreement of mid-winter snowfall increases at high elevations between the two
965 emission scenarios, obvious differences in the spatial extent of the region of mean seasonal snowfall
966 increases can be found (cf Figs. S65 and 7 for δS_{mean} , and Figs. S76 and S87 for δS_{q99}). In most
967 simulations, the number of grid cells along the main Alpine ridge that show either little change or even
968 increases of seasonal mean S_{mean} or S_{q99} is larger for RCP4.5 than for RCP8.5 with its larger warming
969 magnitude.

970 5.3 Intercomparison of projections with separated and raw snowfall

971 The snowfall projections presented above are based on the RCM_{sep+ba} data set, i.e. on separated and
972 bias-adjusted snowfall amounts. To assess the robustness of these estimates we here compare the
973 obtained change signals against the respective signals based on ~~An intercomparison of relative~~
974 ~~change signals for RCM_{sep+bc} (separated and bias-corrected), RCM_{sep+nbae} (separated and not bias-~~
975 ~~corrected/adjusted) and simulated raw snowfall output (RCM_{raw}).~~ based on ~~This comparison is~~
976 restricted to the nine RCMs providing raw snowfall as output variable (see Tab. 1).

977 The three different change estimates agree well with each other In terms of relative snowfall change
978 signals reveals no substantial differences (Fig. 13, top row). ~~In the three data sets, m~~Multi-model mean
979 relative changes are very similar for all analysed snowfall indices and elevation intervals. In many
980 cases, separated and not bias-adjusted snowfall (RCM_{sep+nba}) is subject to slightly smaller percentage
981 decreases. Furthermore, mMulti-model mean differences between RCM_{sep+bac}, RCM_{sep+nbae} and
982 RCM_{raw} simulations are smaller than the corresponding multi-model spread of RCM_{sep+bac} simulations
983 and emission scenario uncertainties (cf. Figs. 12, 13 and S108).

984 This ~~agreement in terms of relative change signals finding~~ is in contrast to absolute change
985 characteristics (Fig. 13, bottom row). Results based on the three data sets agree in the sign of change,
986 but not in their magnitude, especially at high elevations >2000 m a.s.l.. As the relative changes are
987 almost identical, the absolute changes strongly depend upon the treatment of biases in the control
988 climate.

989 -In summary, these findings indicate that (a) the snowfall separation method developed in the present
990 work yields rather good proxies for relative changes of snowfall indices in raw RCM output (which is
991 ~~not available for all for many~~ GCM-RCM chains ~~not available~~), and that (b) the additional bias ~~-~~
992 ~~adjustment correction~~ of separated snowfall amounts only has a weak influence on relative change
993 signals of snowfall indices, but can have substantial effects on absolute changes.

994 **6 Conclusions and outlook**

995 The present work makes use of state-of-the-art EURO-CORDEX RCM simulations to assess changes
996 of snowfall indices over the European Alps by the end of the 21st century. For this purpose, snowfall is
997 separated from total precipitation using near-surface air temperature in both the RCMs and in the an
998 ~~observation-based estimates~~ on a daily basis. The analysis yields a number of robust signals,
999 consistent across a range of climate model chains and across emission scenarios. Relating to the
1000 main objectives we find the following:

1001 **Snowfall separation on an RCM grid.** Binary snow fractionation with a fixed temperature threshold
1002 on coarse-resolution grids (with 11 km resolution) leads to an underestimation of mean snowfall and
1003 an overestimation of heavy snowfall. To overcome these deficiencies, the Richards snow fractionation
1004 method is implemented. This approach expresses that the coarse-grid snow fraction depends not only
1005 on daily mean temperature, but also on topographical subgrid-scale variations. Accounting for the
1006 latter results in better estimates for mean and heavy snowfall. However, due to limited observational
1007 coverage the parameters of this method are fitted for Switzerland only and are then applied to the
1008 entire Alpine domain. Whether this spatial transfer is robust could further be investigated by using
1009 observational data sets covering the full domain of interest but is out of the scope of this study.

1010 **Snowfall bias ~~correction~~ adjustment.** Simulations of the current EURO-CORDEX ensemble are
1011 subject to considerable biases in precipitation and temperature, which translate into biased snowfall
1012 amounts. In the EVAL period, simulated precipitation is largely overestimated, with increasing biases
1013 toward higher altitudes. On the other hand, simulated near surface temperatures are generally too low
1014 with largest deviations over mountainous regions. These findings were already reported in previous
1015 studies for both the current EURO-CORDEX data set but also for previous RCM ensembles (e.g. Frei
1016 et al., 2003; Kotlarski et al., 2012; Kotlarski et al., 2015; Rajczak et al., 2013; Smiatek et al., 2016). By
1017 implementing a simple bias ~~adjustment~~ ~~correction~~ approach, we are able to partly reduce these biases
1018 and the associated model spread, which should enable more robust change estimates. The ~~corrected~~
1019 adjusted model results reproduce the seasonal cycles of mean snowfall fairly well. However,
1020 substantial biases remain in terms of heavy snowfall, snowfall intensities (which in general are
1021 overestimated), snowfall frequencies, and spatial snowfall distributions. Further improvements might

1022 | be feasible by using more sophisticated bias ~~adjustment correction~~ methods, such as quantile
1023 | mapping (e.g., Rajczak et al., 2016), local intensity scaling of precipitation (e.g., Schmidli et al., 2006),
1024 | or weather generators (e.g. Keller et al., 2016). Advantages of the approach employed here are its
1025 | simplicity, its direct linkage to the snowfall separation method and, as a consequence, its potential
1026 | ability to account for non-stationary snowfall biases. Furthermore, a comparison to simulated raw
1027 | snowfall for a subset of nine simulations revealed that relative change signals are almost independent
1028 | of the chosen post-processing strategy.

1029 | **Snowfall projections for the late 21st century.** Snowfall climate change signals are assessed by
1030 | deriving the changes in snowfall indices between the CTRL period 1981 - 2010 and the SCEN period
1031 | 2070 - 2099. Our results show that by the end of the 21st century, snowfall over the Alps will be
1032 | considerably reduced. Between September and May mean snowfall is expected to decrease by
1033 | approximately -45% (multi-model mean) under an RCP8.5 emission scenario. For the more moderate
1034 | RCP4.5 scenario, multi-model mean projections show a decline of -25%. These results are in good
1035 | agreement with previous works (e.g. de Vries et al., 2014; Piazza et al., 2014, Räisänen, 2016). Low-
1036 | lying areas experience the largest percentage changes of more than -80%, while the highest Alpine
1037 | regions are only weakly affected. Variations of heavy snowfall, defined by the 99% all-day snowfall
1038 | percentile, show ~~at low-lying elevations~~ an even more pronounced signal at low-lying elevations. With
1039 | increasing elevation, percentage changes of heavy snowfall are generally smaller than for mean
1040 | snowfall. O'Gorman (2014) found a very similar behaviour by analysing projected changes in mean
1041 | and extreme snowfall over the entire Northern Hemisphere. He pointed out that heavy and extreme
1042 | snowfall occurs near an optimal temperature (near or below freezing, but not too cold), which seems to
1043 | be independent of climate warming. We here confirm this ~~conclusion finding~~. At mid and high
1044 | elevations ~~the optimal temperature for~~ heavy snowfall in a warmer climate will still occur in ~~a warmer~~
1045 | ~~climate the optimal temperature range~~ and, hence, heavy snowfall amounts will decrease less strongly
1046 | compared to mean snowfall, and may even increase in some areas.:-

1047 | At first approximation, the magnitude of future warming strongly influences the reduction of mean and
1048 | heavy snowfall by modifying the snowfall frequency. Snowfall increases may however occur at high
1049 | (and thus cold) elevations, and these are not caused by frequency changes. Here, snowfall increases
1050 | due to (a) a general increase of total winter precipitation combined with only minor changes in snowfall
1051 | frequency, and (b) more intense snowfall. This effect has a pronounced altitudinal distribution and may
1052 | be particularly strong under conditions (depending upon location and season) where the current
1053 | climate is well below freezing. Such conditions may experience a shift towards a ~~more snowfall-~~
1054 | ~~friendly~~ temperature range more favourable to snowfall (near or below freezing, but not too cold) with
1055 | corresponding increases of mean snowfall, despite a general decrease of the snowfall fraction.

1056 | The identified future changes of snowfall over the Alps can lead to a variety of impacts in different
1057 | sectors. With decreasing snowfall frequencies and the general increase of the snowline (e.g.,
1058 | Beniston, 2003; Gobiet et al., 2014; Hantel et al., 2012), both associated with temperature changes,
1059 | ski lift operators are looking into an uncertain future. A shorter snowfall season will likely put them
1060 | under greater financial pressure. Climate change effects might be manageable only for ski areas

1061 reaching up to high elevations (e.g. Elsasser and Bürki, 2002). Even so these resorts might start later
1062 into the ski season, the snow conditions into early spring could change less dramatically due to
1063 projected high-elevation snowfall increases in mid-winter. A positive aspect of the projected decrease
1064 in snowfall frequency might be a reduced expenditures for airport and road safety (e.g., Zubler et al.,
1065 2015).

1066 At lower altitudes, an intensification of winter precipitation, combined with smaller snowfall fractions
1067 (Serquet et al., 2013), increases the flood potential (Beniston, 2012). Snow can act as a buffer by
1068 releasing melt water constantly over a longer period of time. With climate warming, this storage
1069 capacity is lost, and heavy precipitation immediately drains into streams and rivers which might not be
1070 able to take up the vast amount of water fast enough. Less snowmelt will also have impacts on
1071 hydropower generation and water management (e.g., Weingartner et al., 2013). So far, many Alpine
1072 regions are able to bypass dry periods by tapping melt water from mountainous regions. With reduced
1073 snow-packs due to less snowfall, water shortage might become a serious problem in some areas.

1074 Regarding specific socio-economic impacts caused by extreme snowfall events, conclusions based on
1075 the results presented in this study are difficult to draw. It might be possible that the 99% all-day
1076 snowfall percentile we used for defining heavy snowfalls, is not appropriate to speculate about future
1077 evolutions of (very) rare events (Schär et al., 2016). To do so, one might consider applying a
1078 generalized extreme value (GEV) analysis which is more suitable for answering questions related to
1079 rare extreme events.

1080 **7 Data Availability**

1081 The EURO-CORDEX RCM data analysed in the present work are publicly available - parts of
1082 them for non-commercial use only - via the Earth System Grid Federation archive (ESGF;
1083 e.g., <https://esgf-data.dkrz.de>). The observational datasets RHiresD and TabsD as well as
1084 the snow depth data for Switzerland are available for research and educational purposes
1085 from kundendienst@meteoschweiz.ch. The analysis code is available from the
1086 corresponding author on request.

1087 **8 Competing Interests**

1088 The authors declare that they have no conflict of interest.

1089 **9 Acknowledgements**

1090 We gratefully acknowledge the support of Jan Rajczak, Urs Beyerle and Curdin Spirig (ETH Zurich) as
1091 well as Elias Zubler (MeteoSwiss) in data acquisition and pre-processing. Christoph Frei (MeteoSwiss)
1092 and Christoph Marty (WSL-SLF) provided important input on specific aspects of the analysis. [The](#)
1093 [GTOPO30 digital elevation model is available from the U.S. Geological Survey.](#) Finally, we thank the

1094 climate modelling groups of the EURO-CORDEX initiative for producing and making available their
1095 model output.

1096 **10 References**

- 1097 Abegg, B. A., S., Crick, F., and de Montfalcon, A.: Climate change impacts and adaptation in winter tourism, in:
1098 Climate change in the European Alps: adapting winter tourism and natural hazards management, edited by:
1099 Agrawala, S., Organisation for Economic Cooperation and Development (OECD), Paris, France, 25-125, 2007.
- 1100 Allen, M. R., and Ingram, W. J.: Constraints on future changes in climate and the hydrologic cycle, *Nature*, 419,
1101 224-232, 10.1038/nature01092, 2002.
- 1102 Ban, N., Schmidli, J., and Schär, C.: Heavy precipitation in a changing climate: Does short-term summer
1103 precipitation increase faster?, *Geophys Res Lett*, 42, 1165-1172, 10.1002/2014GL062588, 2015.
- 1104 Beniston, M.: Climatic Change in Mountain Regions: A Review of Possible Impacts. *Clim Change*, 59, 5-31.
- 1105 Beniston, M.: Impacts of climatic change on water and associated economic activities in the Swiss Alps, *J Hydrol*,
1106 412, 291-296, 10.1016/j.jhydrol.2010.06.046, 2012.
- 1107 [Ceppi, P., Scherrer, S.C., Fischer, A.M., and Appenzeller, C.: Revisiting Swiss temperature trends 1959–2008, *Int*
1108 *J Climatol*, 32, 203-213, 10.1002/joc.2260, 2012.](#)
- 1109 CH2011: Swiss Climate Change Scenarios CH2011, published by C2SM, MeteoSwiss, ETH, NCCR Climate, and
1110 OcCC, Zurich, Switzerland, 88 pp, 2011.
- 1111 [Chimani, B., Böhm, R., Matulla, C., and Ganekind, M.: Development of a longterm dataset of solid/liquid
1112 precipitation, *Adv Sci Res*, 6, 39-43, 10.5194/asr-6-39-2011, 2011.](#)
- 1113 de Vries, H., Haarsma, R. J., Hazeleger, W.: On the future reduction of snowfall in western and central Europe.
1114 *Clim Dyn*, 41, 2319-2330, 10.1007/s00382-012-1583-x, 2013.
- 1115 de Vries, H., Lenderink, G., and van Meijgaard, E.: Future snowfall in western and central Europe projected with a
1116 high-resolution regional climate model ensemble, *Geophys Res Lett*, 41, 4294-4299, 10.1002/2014GL059724,
1117 2014.
- 1118 Deser, C., Knutti, R., Solomon, S. and Phillips, A. S.: Communication of the role of natural variability in future
1119 North American climate. *Nature Clim Change*, 2, 775-779, 2012.
- 1120 Elsasser, H. and Bürki, R.: Climate change as a threat to tourism in the Alps. *Climate Research*, 20, 253-257.
- 1121 Fischer, A. M., Keller, D. E., Liniger, M. A., Rajczak, J., Schär, C., and Appenzeller, C.: Projected changes in
1122 precipitation intensity and frequency in Switzerland: a multi-model perspective, *Int J Climatol*, 35, 3204-3219,
1123 10.1002/joc.4162, 2015.
- 1124 Fischer, E. M. and Knutti, R.: Observed heavy precipitation increase confirms theory and early models. *Nature*
1125 *Clim Change*, 6, 986-992, 10.1038/NCLIMATE3110, 2016.
- 1126 Frei, C. and Schär, C.: A precipitation climatology of the Alps from high-resolution rain-gauge observations, *Int J*
1127 *Climatol*, 18, 873-900, 10.1002/(Sici)1097-0088(19980630)18:8<873::Aid-Joc255>3.0.Co;2-9, 1998.
- 1128 Frei, C., Christensen, J. H., Déqué, M., Jacob, D., Jones, R. G., and Vidale, P. L.: Daily precipitation statistics in
1129 regional climate models: Evaluation and intercomparison for the European Alps, *J Geophys Res-Atmos*, 108,
1130 10.1029/2002jd002287, 2003.
- 1131 Frei, C.: Interpolation of temperature in a mountainous region using nonlinear profiles and non-Euclidean
1132 distances, *Int J Climatol*, 34, 1585-1605, 10.1002/joc.3786, 2014.
- 1133 Giorgi, F.: Simulation of regional climate using a limited area model nested in a general circulation model, *J*
1134 *Climate*, 3, 941-963, 1990.
- 1135 Giorgi, F., Jones, C., and Asrar, G. R.: Addressing climate information needs at the regional level: the CORDEX
1136 framework, *World Meteorological Organization (WMO) Bulletin*, 58, 175, 2009.
- 1137 Giorgi, F., Torma, C., Coppola, E., Ban, N., Schär, C., and Somot, S.: Enhanced summer convective rainfall at
1138 Alpine high elevations in response to climate warming, *Nat Geo*, 9, 584-589, 10.1038/ngeo2761, 2016.
- 1139 Gobiet, A., Kotlarski, S., Beniston, M., Heinrich, G., Rajczak, J., and Stoffel, M.: 21st century climate change in
1140 the European Alps - A review, *Science of the Total Environment*, 493, 1138-1151,
1141 10.1016/j.scitotenv.2013.07.050, 2014.
- 1142 [Grünewald, T., and Lehning, M.: Are flat-field snow depth measurements representative? A comparison of
1143 selected index sites with areal snow depth measurements at the small catchment scale, *Hydrol Processes*, 29,
1144 1717-1728, 10.1002/hyp.10295, 2015.](#)

- 1145 Hantel, M., Maurer, C., and Mayer, D.: The snowline climate of the Alps 1961–2010. *Theor Appl Climatol*, 110,
1146 517, 10.1007/s00704-012-0688-9, 2012.
- 1147 Hawkins, E., and Sutton, R.: The Potential to Narrow Uncertainty in Regional Climate Predictions, *B Am Meteorol*
1148 *Soc*, 90, 1095–+, 10.1175/2009BAMS2607.1, 2009.
- 1149 Haylock, M.R., Hofstra, N., Klein Tank, A.M.G., Klok, E.J., Jones, P.D., and New, M.: A European daily high-
1150 resolution gridded data set of surface temperature and precipitation for 1950–2006, *J Geophys Res*, 113,
1151 D20119, 10.1029/2008JD010201.
- 1152 Held, I. M., and Soden, B. J.: Robust responses of the hydrological cycle to global warming, *J Climate*, 19, 5686-
1153 5699, 10.1175/Jcli3990.1, 2006.
- 1154 IPCC: Climate Change 2013: The Physical Science Basis. Contribution of Working Group I to the Fifth
1155 Assessment Report of the Intergovernmental Panel on Climate Change, Cambridge University Press, Cambridge,
1156 United Kingdom and New York, NY, USA, 1535 pp., 2013.
- 1157 Isotta, F. A., Frei, C., Weilguni, V., Tadic, M. P., Lassegues, P., Rudolf, B., Pavan, V., Cacciamani, C., Antolini,
1158 G., Ratto, S. M., Munari, M., Micheletti, S., Bonati, V., Lussana, C., Ronchi, C., Panettieri, E., Marigo, G., and
1159 Vertacnik, G.: The climate of daily precipitation in the Alps: development and analysis of a high-resolution grid
1160 dataset from pan-Alpine rain-gauge data, *Int J Climatol*, 34, 1657-1675, 10.1002/joc.3794, 2014.
- 1161 Jacob, D., Petersen, J., Eggert, B., Alias, A., Christensen, O. B., Bouwer, L. M., Braun, A., Colette, A., Déqué, M.,
1162 Georgievski, G., Georgopoulou, E., Gobiet, A., Menut, L., Nikulin, G., Haensler, A., Hempelmann, N., Jones, C.,
1163 Keuler, K., Kovats, S., Kröner, N., Kotlarski, S., Kriegsman, A., Martin, E., van Meijgaard, E., Moseley, C.,
1164 Pfeifer, S., Preuschmann, S., Radermacher, C., Radtke, K., Rechid, D., Rounsevell, M., Samuelsson, P., Somot,
1165 S., Soussana, J. F., Teichmann, C., Valentini, R., Vautard, R., Weber, B., and Yiou, P.: EURO-CORDEX: new
1166 high-resolution climate change projections for European impact research, *Reg Environ Change*, 14, 563-578,
1167 10.1007/s10113-013-0499-2, 2014.
- 1168 Keller, D. E., Fischer, A. M., Liniger, M. A., Appenzeller, C. and Knutti, R.: Testing a weather generator for
1169 downscaling climate change projections over Switzerland. *Int J Climatol*, doi:10.1002/joc.4750, 2016.
- 1170 Kienzle, S. W.: A new temperature based method to separate rain and snow, *Hydrol Process*, 22, 5067-5085,
1171 10.1002/hyp.7131, 2008.
- 1172 [Kotlarski, S., Bosshard, T., Lüthi, D., Pall, P., and Schär, C.: Elevation gradients of European climate change in
1173 the regional climate model COSMO-CLM. *Clim Change*, 112, 189-215, 10.1007/s10584-011-0195-5, 2012.](#)
- 1174 Kotlarski, S., Keuler, K., Christensen, O. B., Colette, A., Deque, M., Gobiet, A., Goergen, K., Jacob, D., Luthi, D.,
1175 van Meijgaard, E., Nikulin, G., Schar, C., Teichmann, C., Vautard, R., Warrach-Sagi, K., and Wulfmeyer, V.:
1176 Regional climate modeling on European scales: a joint standard evaluation of the EURO-CORDEX RCM
1177 ensemble, *Geosci Model Dev*, 7, 1297-1333, 10.5194/gmd-7-1297-2014, 2014.
- 1178 Kotlarski, S., Lüthi, D., and Schär, C.: The elevation dependency of 21st century European climate change: an
1179 RCM ensemble perspective, *Int J Climatol*, 35, 3902-3920, 10.1002/joc.4254, 2015.
- 1180 Krasting, J. P., Broccoli, A. J., Dixon, K. W., and Lanzante, J. R.: Future Changes in Northern Hemisphere
1181 Snowfall. *J Clim*, 26, 7813-7828, 10.1175/JCLI-D-12-00832.1, 2013.
- 1182 Laternser, M., and Schneebeli, M.: Long-term snow climate trends of the Swiss Alps (1931-99), *Int J Climatol*, 23,
1183 733-750, 10.1002/joc.912, 2003.
- 1184 Marty, C.: Regime shift of snow days in Switzerland, *Geophys Res Lett*, 35, 10.1029/2008gl033998, 2008.
- 1185 Marty, C., and Blanchet, J.: Long-term changes in annual maximum snow depth and snowfall in Switzerland
1186 based on extreme value statistics, *Climatic Change*, 111, 705-721, 2011.
- 1187 McAfee, S. A., Walsh, J., and Rupp, T. S.: Statistically downscaled projections of snow/rain partitioning for
1188 Alaska, *Hydrol Process*, 28, 3930-3946, 10.1002/hyp.9934, 2014.
- 1189 [MeteoSchweiz: Klimareport 2015. Bundesamt für Meteorologie und Klimatologie MeteoSchweiz, Zürich.](#)
- 1190 MeteoSwiss: Daily Precipitation (final analysis): RhiresD:
1191 [www.meteoswiss.admin.ch/content/dam/meteoswiss/de/service-und-publikationen/produkt/raeumliche-daten-](http://www.meteoswiss.admin.ch/content/dam/meteoswiss/de/service-und-publikationen/produkt/raeumliche-daten-niederschlag/doc/ProdDoc_RhiresD.pdf)
1192 [niederschlag/doc/ProdDoc_RhiresD.pdf](http://www.meteoswiss.admin.ch/content/dam/meteoswiss/de/service-und-publikationen/produkt/raeumliche-daten-niederschlag/doc/ProdDoc_RhiresD.pdf), access: 10.01.2017, 2013a.
- 1193 MeteoSwiss: Daily Mean, Minimum and Maximum Temperature: TabsD, TminD, TmaxD:
1194 [www.meteoswiss.admin.ch/content/dam/meteoswiss/de/service-und-publikationen/produkt/raeumliche-daten-](http://www.meteoswiss.admin.ch/content/dam/meteoswiss/de/service-und-publikationen/produkt/raeumliche-daten-temperatur/doc/ProdDoc_TabsD.pdf)
1195 [temperatur/doc/ProdDoc_TabsD.pdf](http://www.meteoswiss.admin.ch/content/dam/meteoswiss/de/service-und-publikationen/produkt/raeumliche-daten-temperatur/doc/ProdDoc_TabsD.pdf), access: 10.01.2017, 2013b.
- 1196 Moss, R. H., Edmonds, J. A., Hibbard, K. A., Manning, M. R., Rose, S. K., van Vuuren, D. P., Carter, T. R., Emori,
1197 S., Kainuma, M., Kram, T., Meehl, G. A., Mitchell, J. F. B., Nakicenovic, N., Riahi, K., Smith, S. J., Stouffer, R. J.,
1198 Thomson, A. M., Weyant, J. P., and Wilbanks, T. J.: The next generation of scenarios for climate change research
1199 and assessment, *Nature*, 463, 747-756, 10.1038/nature08823, 2010.

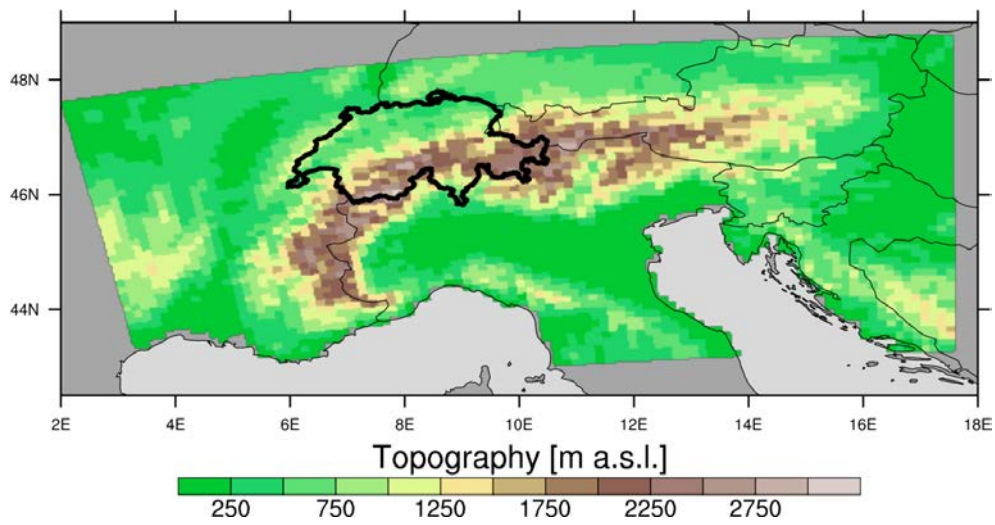
- 1200 Neff, E. L.: How Much Rain Does a Rain Gauge Gauge, *J Hydrol*, 35, 213-220, 10.1016/0022-1694(77)90001-4,
1201 1977.
- 1202 O'Gorman, P. A.: Contrasting responses of mean and extreme snowfall to climate change, *Nature*, 512, 416-
1203 U401, 10.1038/nature13625, 2014.
- 1204 Piazza, M., Boé, J., Terray, L., Pagé, C., Sanchez-Gomez, E., and Déqué, M.: Projected 21st century snowfall
1205 changes over the French Alps and related uncertainties, *Climatic Change*, 122, 583-594, 10.1007/s10584-013-
1206 1017-8, 2014.
- 1207 Räisänen, J.: Twenty-first century changes in snowfall climate in Northern Europe in ENSEMBLES regional
1208 climate models, *Clim Dynam*, 46, 339-353, 10.1007/s00382-015-2587-0, 2016.
- 1209 Rajczak, J., Pall, P., and Schär, C.: Projections of extreme precipitation events in regional climate simulations for
1210 Europe and the Alpine Region, *J Geophys Res-Atmos*, 118, 3610-3626, 10.1002/jgrd.50297, 2013.
- 1211 Rajczak, J., Kotlarski, S., and Schär, C.: Does Quantile Mapping of Simulated Precipitation Correct for Biases in
1212 Transition Probabilities and Spell Lengths?, *J Climate*, 29, 1605-1615, 10.1175/Jcli-D-15-0162.1, 2016.
- 1213 Rajczak, J. and Schär, C.: Projections of future precipitation extremes over Europe: A multi-model assessment of
1214 climate simulations. In preparation.
- 1215 Richards, F. J.: A Flexible Growth Function for Empirical Use, *J Exp Bot*, 10, 290-300, 10.1093/Jxb/10.2.290,
1216 1959.
- 1217 Rummukainen, M.: State-of-the-art with regional climate models, *Wiley Interdisciplinary Reviews-Climate Change*,
1218 1, 82-96, 10.1002/wcc.8, 2010.
- 1219 Schär, C., Ban, N., Fischer, E. M., Rajczak, J., Schmidli, J., Frei, C., Giorgi, F., Karl, T. R., Kendon, E. J., Tank, A.
1220 M. G. K., O'Gorman, P. A., Sillmann, J., Zhang, X. B., and Zwiers, F. W.: Percentile indices for assessing changes
1221 in heavy precipitation events, *Climatic Change*, 137, 201-216, 10.1007/s10584-016-1669-2, 2016.
- 1222 Scherrer, S. C., Appenzeller, C., and Laternser, M.: Trends in Swiss Alpine snow days: The role of local- and
1223 large-scale climate variability, *Geophys Res Lett*, 31, 10.1029/2004gl020255, 2004.
- 1224 Schmidli, J., Frei, C., and Vidale, P. L.: Downscaling from GCM precipitation: A benchmark for dynamical and
1225 statistical downscaling methods, *Int J Climatol*, 26, 679-689, 10.1002/joc.1287, 2006.
- 1226 Schmucki, E., Marty, C., Fierz, C., and Lehning, M.: Simulations of 21st century snow response to climate change
1227 in Switzerland from a set of RCMs, *Int J Climatol*, 35, 3262-3273, 10.1002/joc.4205, 2015a.
- 1228 Schmucki, E., Marty, C., Fierz, C., Weingartner, R. and Lehning, M.: Impact of climate change in Switzerland on
1229 socioeconomic snow indices, *Theor Appl Climatol*, in press, 10.1007/s00704-015-1676-7, 2015b.
- 1230 Serquet, G., Marty, C., and Rebetez, M.: Monthly trends and the corresponding altitudinal shift in the
1231 snowfall/precipitation day ratio, *Theor Appl Climatol*, 114, 437-444, 10.1007/s00704-013-0847-7, 2013. Sevruck, B.:
1232 Der Niederschlag in der Schweiz, Geographisches Institut der Eidgenössischen Technischen Hochschule in
1233 Zürich, Abteilung Hydrologie, Zurich, Switzerland, 1985.
- 1234 SFOE, Hydropower: <http://www.bfe.admin.ch/themen/00490/00491/index.html?lang=en>, access: 16.09.2016,
1235 2014.
- 1236 Smiatek, G., Kunstmann, H., and Senatore, A.: EURO-CORDEX regional climate model analysis for the Greater
1237 Alpine Region: Performance and expected future change, *J Geophys Res-Atmos*, 121, 7710-7728,
1238 10.1002/2015JD024727, 2016.
- 1239 Soncini, A., and Bocchiola, D.: Assessment of future snowfall regimes within the Italian Alps using general
1240 circulation models, *Cold Reg Sci Technol*, 68, 113-123, 10.1016/j.coldregions.2011.06.011, 2011.
- 1241 Steger, C., Kotlarski, S., Jonas, T., and Schär, C.: Alpine snow cover in a changing climate: a regional climate
1242 model perspective, *Clim Dynam*, 41, 735-754, 10.1007/s00382-012-1545-3, 2013.
- 1243 Techel, F., Stucki, T., Margreth, S., Marty, C., and Winkler, K.: Schnee und Lawinen in den Schweizer Alpen.
1244 Hydrologisches Jahr 2013/14, WSL-Institut für Schnee- und Lawinenforschung SLF, Birmensdorf, Switzerland,
1245 2015.
- 1246 Terzago, S., von Hardenberg, J., Palazzi, E., and Provenzale, A.: Snow water equivalent in the Alps as seen by
1247 gridded datasets, CMIP5 and CORDEX climate models. *The Cryosphere Discussion*, 10.5194/tc-2016-280, 2017.
- 1248 Torma, C., Giorgi, F., and Coppola, E.: Added value of regional climate modeling over areas characterized by
1249 complex terrain Precipitation over the Alps, *J Geophys Res-Atmos*, 120, 3957-3972, 10.1002/2014JD022781,
1250 2015.
- 1251 Vautard, R., Gobiet, A., Jacob, D., Belda, M., Colette, A., Déqué, M., Fernandez, J., Garcia-Diez, M., Goergen,
1252 K., Guttler, I., Halenka, T., Karacostas, T., Katragkou, E., Keuler, K., Kotlarski, S., Mayer, S., van Meijgaard, E.,
1253 Nikulin, G., Patarcic, M., Scinocca, J., Sobolowski, S., Suklitsch, M., Teichmann, C., Warrach-Sagi, K.,
1254 Wulfmeyer, V., and Yiou, P.: The simulation of European heat waves from an ensemble of regional climate
1255 models within the EURO-CORDEX project, *Clim Dynam*, 41, 2555-2575, 10.1007/s00382-013-1714-z, 2013.

- 1256 Weingartner, R., Schädler, B., and Hänggi, P.: Auswirkungen der Klimaänderung auf die schweizerische
1257 Wasserkraftnutzung, *Geographica Helvetica*, 68, 239-248, 2013.
- 1258 Yang, D. Q., Elomaa, E., Tuominen, A., Aaltonen, A., Goodison, B., Gunther, T., Golubev, V., Sevruk, B.,
1259 Madsen, H., and Milkovic, J.: Wind-induced precipitation undercatch of the Hellmann gauges, *Nord Hydrol*, 30,
1260 57-80, 1999.
- 1261 Zubler, E. M., Scherrer, S. C., Croci-Maspoli, M., Liniger, M. A., and Appenzeller, C.: Key climate indices in
1262 Switzerland; expected changes in a future climate, *Climatic Change*, 123, 255-271, 10.1007/s10584-013-1041-8,
1263 2014.
- 1264 Zubler, E. M., Fischer, A. M., Liniger, M. A., and Schlegel, T.: Auftausalzverbrauch im Klimawandel, MeteoSwiss,
1265 Zurich, Switzerland, Fachbericht 253, 2015.
- 1266

1267 **Figures**

1268

1269

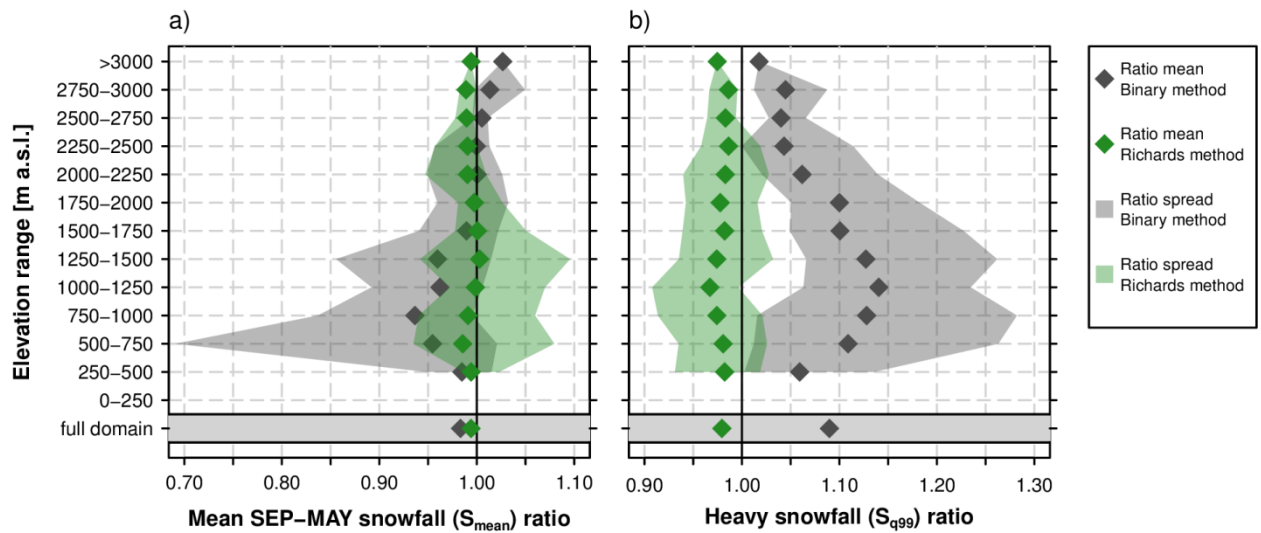


1270

1271

1272 **Figure 1** GTOPO30 ~~t~~Topography (<https://ita.cr.usgs.gov/GTOPO30>) aggregated to the ~~at~~EUR-11 (0.11°) RCM
1273 grid. ~~resolution of~~ ~~The coloured area shows~~ the Alpine domain used for the assessment of snowfall projections.
1274 The bold black outline marks the Swiss sub-domain used for the assessment of the bias adjustment~~correction~~
1275 approach.

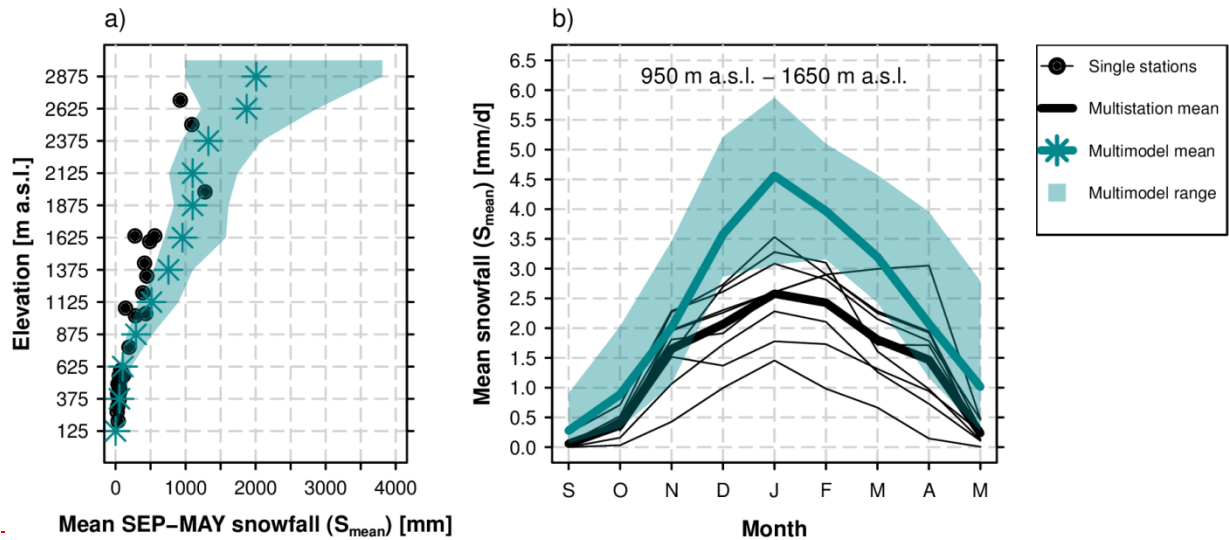
1276



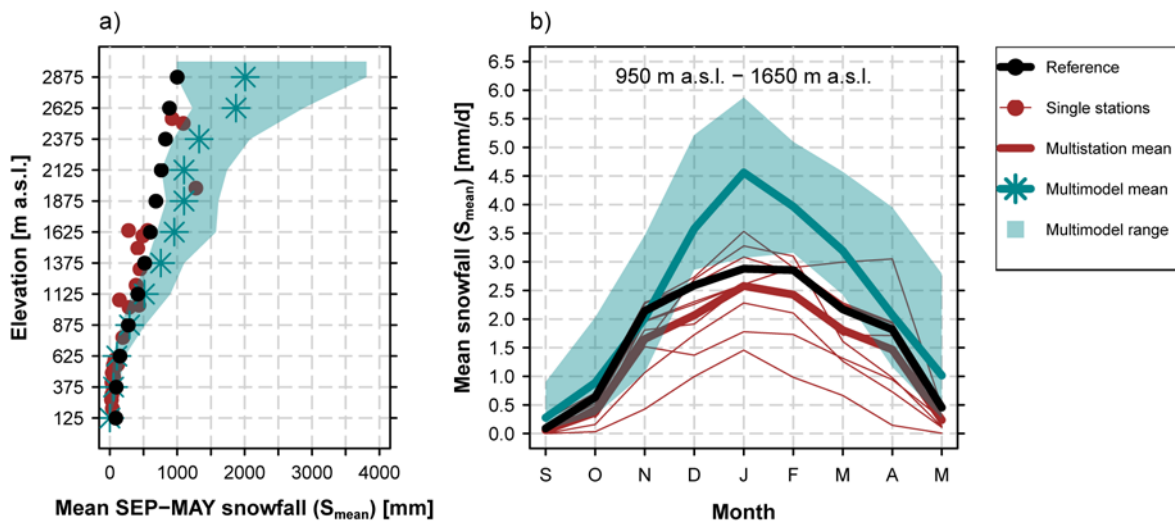
1277
1278

1279 | **Figure 2** Snowfall ratios for the Binary and Richards snow fractionation method (ratio between the snowfall of the
 1280 | respective method and the ~~full-subgrid-snow-representation~~ Subgrid method). The ratios are valid at the coarse-
 1281 | resolution grid (12 km). a) Ratios for mean snowfall, S_{mean} . b) Ratios for heavy snowfall, S_{q99} . Ratio means were
 1282 | derived after averaging the corresponding snowfall index for 250 m elevation intervals in Switzerland while the
 1283 | ratio spread represents the minimum and maximum grid point-based ratios in the corresponding elevation
 1284 | interval. This analysis is entirely based on the observational data sets TabsD and RhiresD.

1285



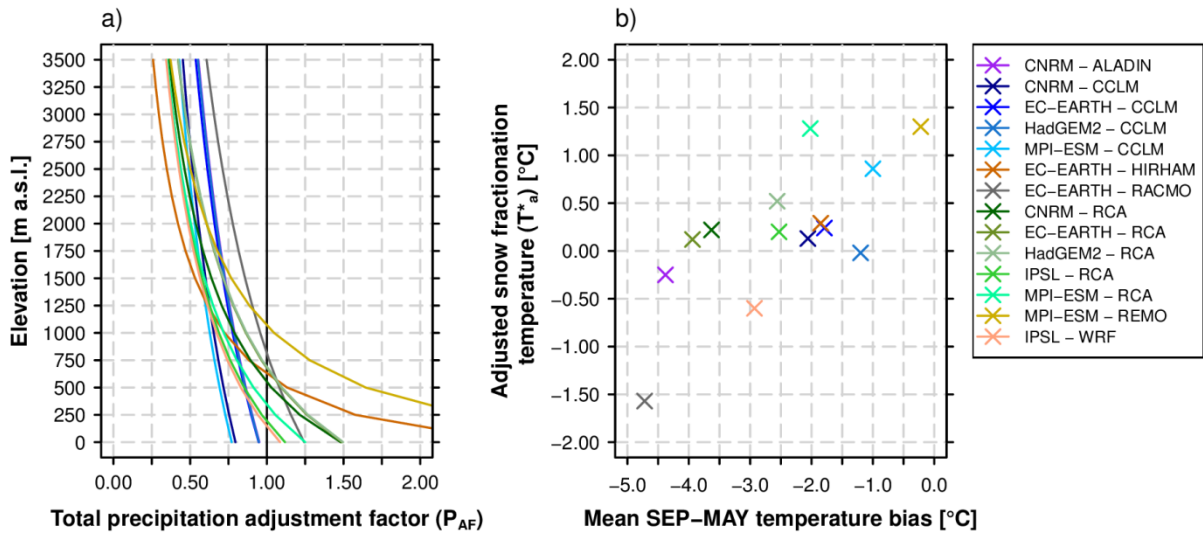
1286



1287

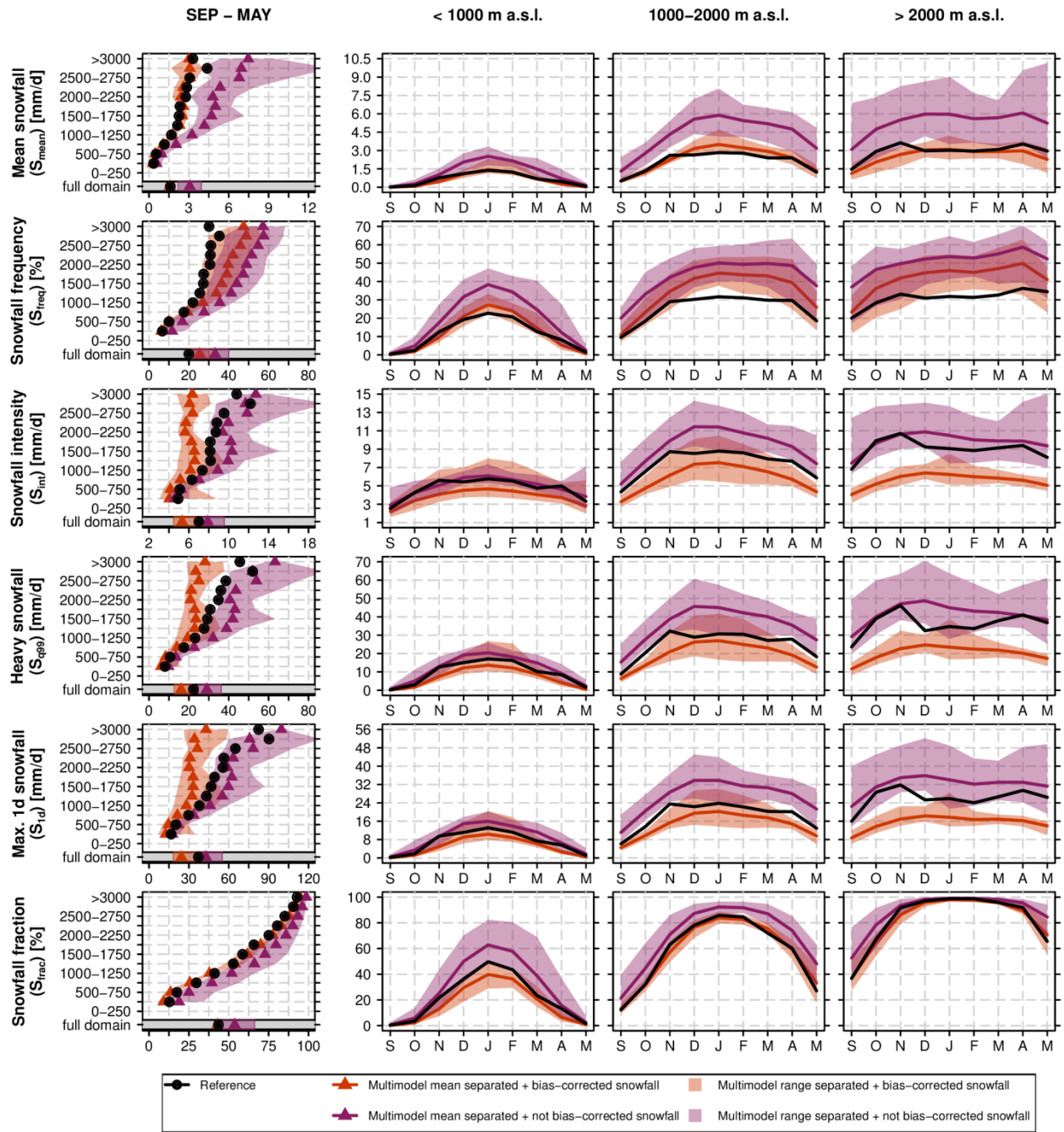
1288 **Figure 3** Comparison of measured fresh snow sums of 29 MeteoSwiss stations (red) against vs. simulated RCM
 1289 raw snowfall in Switzerland (green) and against the 2 km reference snowfall grid obtained by employing the
 1290 Subgrid method (black) in the EVAL period 1971-2005. a) Mean September – May snowfall vs. elevation. Both
 1291 the simulation data (green) and the reference data (black) are based on the spatio-temporal mean of 250 m
 1292 elevation ranges and plotted at the mean elevation of the corresponding interval. b) Seasonal September-May
 1293 snowfall cycle for the elevation interval 950 m a.s.l. to 1650 m a.s.l.. Simulated multi-model means and spreads
 1294 are based on a subset of 9 EURO-CORDEX simulations providing raw snowfall as output variable (see Tab. 1).

1295



1296
1297

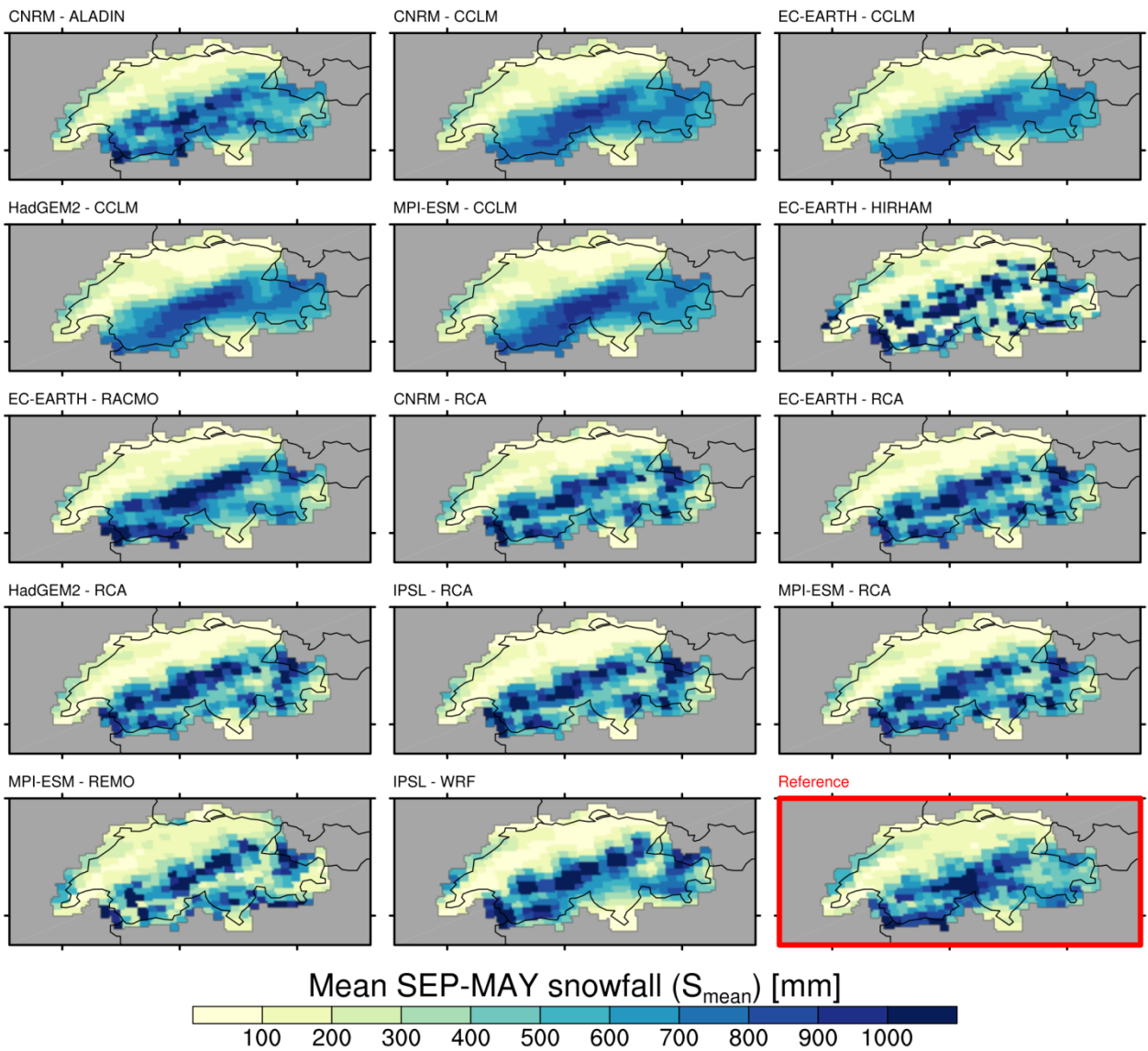
1298 | **Figure 4** ~~Bias correction and adjustment factors~~ Overview on bias adjustment. a) Elevation-dependent total
1299 precipitation adjustment factors, P_{AF} , for the 14 GCM-RCM chains (see Eq. 10). b) Scatterplot of mean September
1300 to May temperature biases (RCM simulation minus observational analysis) vs. adjusted snow fractionation
1301 temperatures, T^*_a .



1302
1303

1304 **Figure 5** Evaluation of snowfall indices in the EVAL period 1971-2005 for the 14 snowfall separated + bias-
 1305 corrected-adjusted ($RCM_{sep+bae}$) and 14 snowfall separated + not bias-corrected-adjusted ($RCM_{sep+nb_{ae}}$) RCM
 1306 simulations vs. observation-based reference. The first column shows the mean September-May snowfall index
 1307 statistics vs. elevation while the monthly snowfall indices (spatially averaged over the elevation intervals <1000
 1308 m.a.s.l., 1000 m a.s.l.-2000 m a.s.l. and >2000 m a.s.l.) are displayed in columns 2-4.

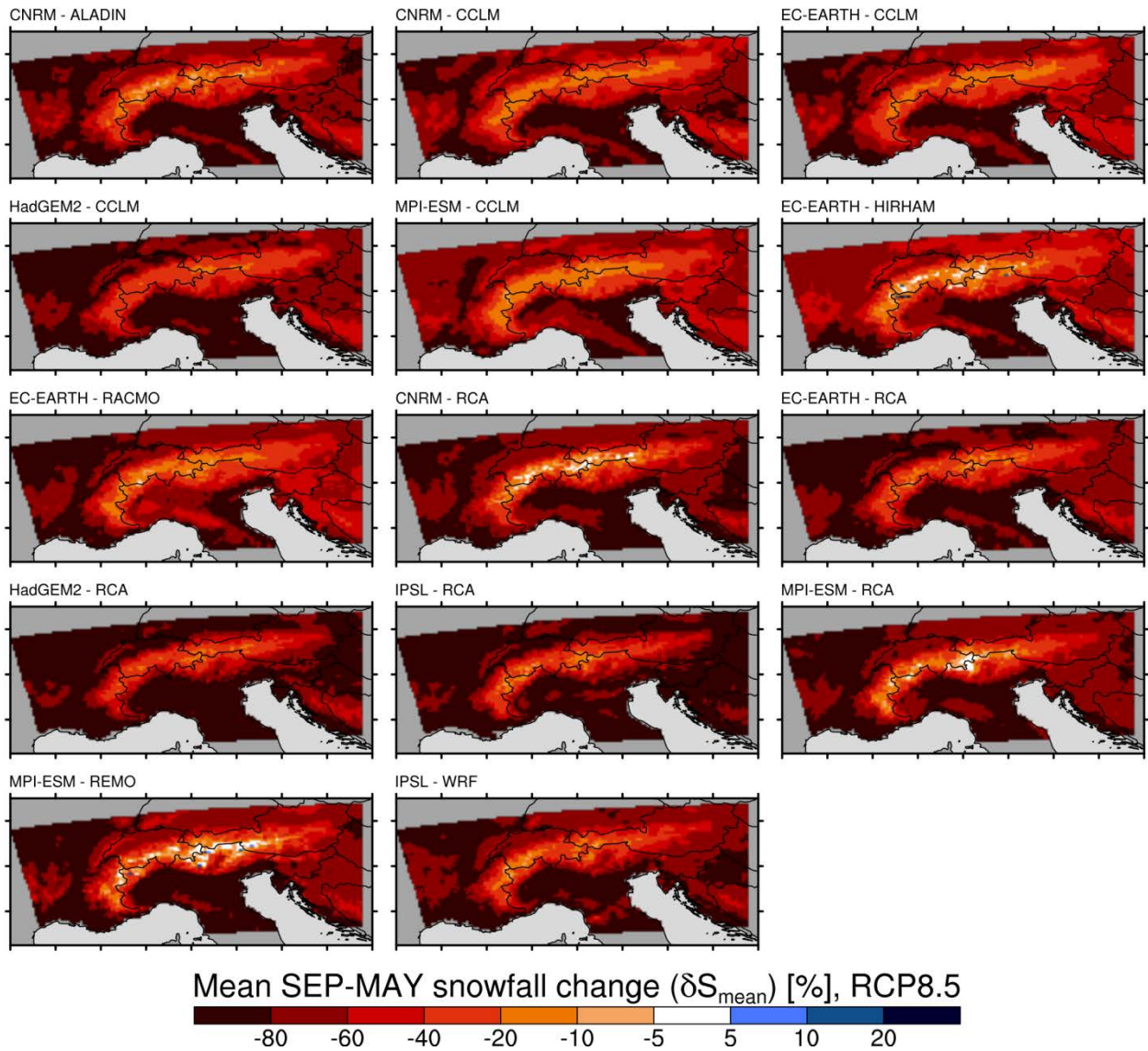
1309



1310
1311

1312 **Figure 6** Spatial distribution of mean September-May snowfall, S_{mean} , in the EVAL period 1971-2005 and for the
 1313 | 14 snowfall separated + bias-~~corrected~~-adjusted RCM simulations ($\text{RCM}_{\text{sep}+\text{bae}}$). In the lower right panel, the map
 1314 of the observation-based reference is shown.

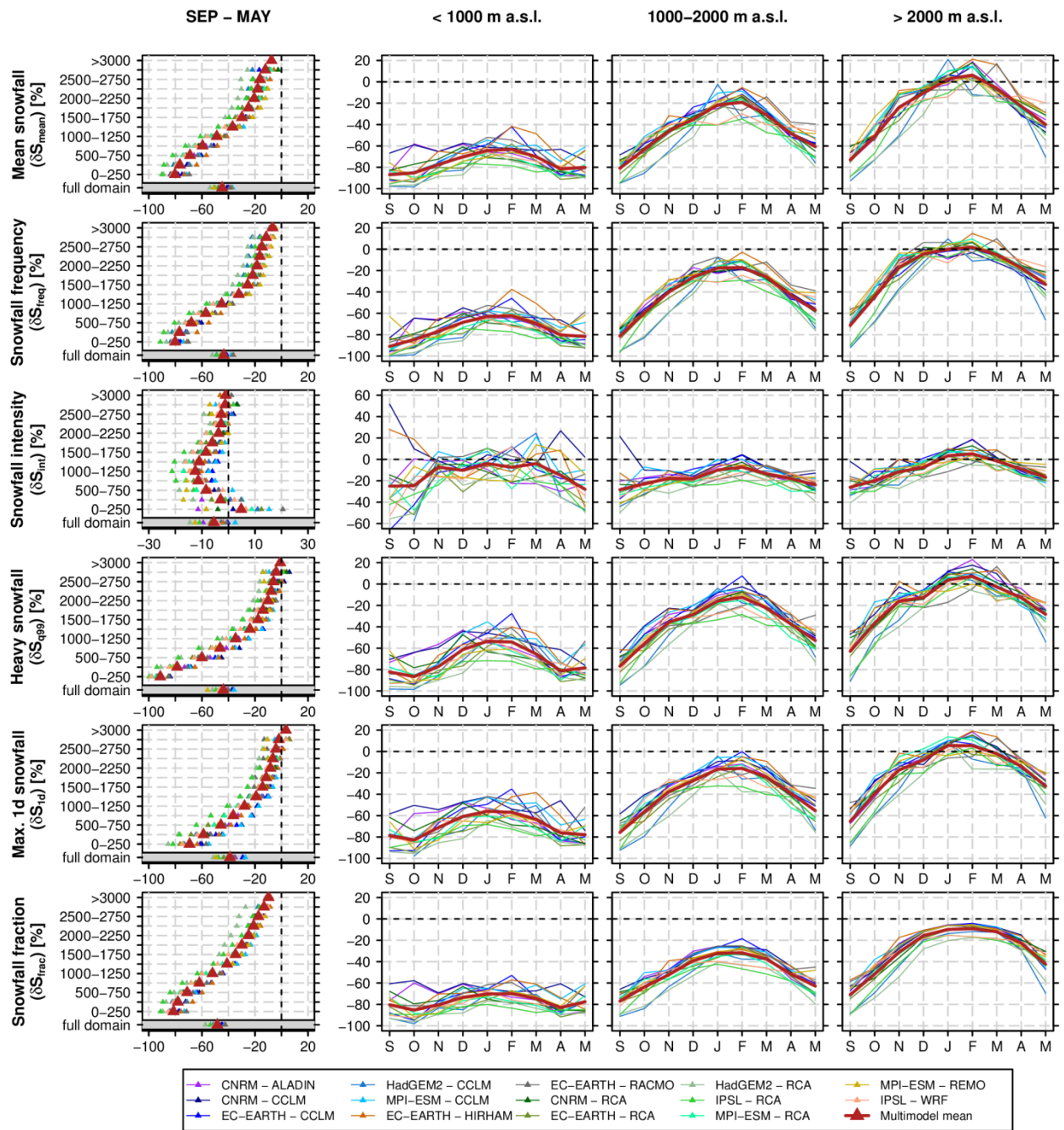
1315



1316
1317

1318 **Figure 7** Spatial distribution of relative changes (SCEN period 2070-2099 with respect to CTRL period 1981-
 1319 2010) in mean September-May snowfall, δS_{mean} , for RCP8.5 and for the 14 snowfall separated + bias_corrected
 1320 adjusted RCM simulations ($\text{RCM}_{\text{sep+b}_{\text{ae}}}$). For RCP4.5, see Fig. S65.

1321

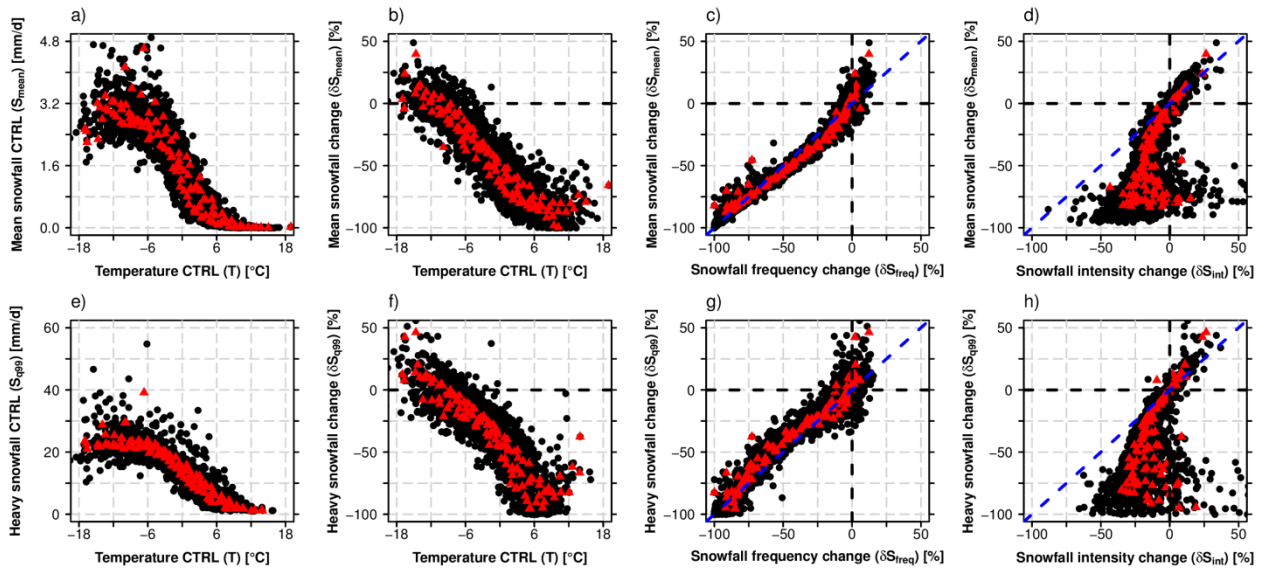


1322

1323

1324 **Figure 8** Relative changes (SCEN period 2070-2099 with respect to CTRL period 1981-2010) of snowfall indices
 1325 based on the 14 snowfall separated + bias-~~corrected~~-~~adjusted~~ RCM simulations ($RCM_{\text{sep+bag}}$) for RCP8.5. The
 1326 first column shows the mean September-May snowfall index statistics vs. elevation while monthly snowfall index
 1327 changes (spatially averaged over the elevation intervals <1000 m.a.s.l., 1000 m a.s.l.-2000 m a.s.l. and >2000 m
 1328 a.s.l.) are displayed in columns 2-4.

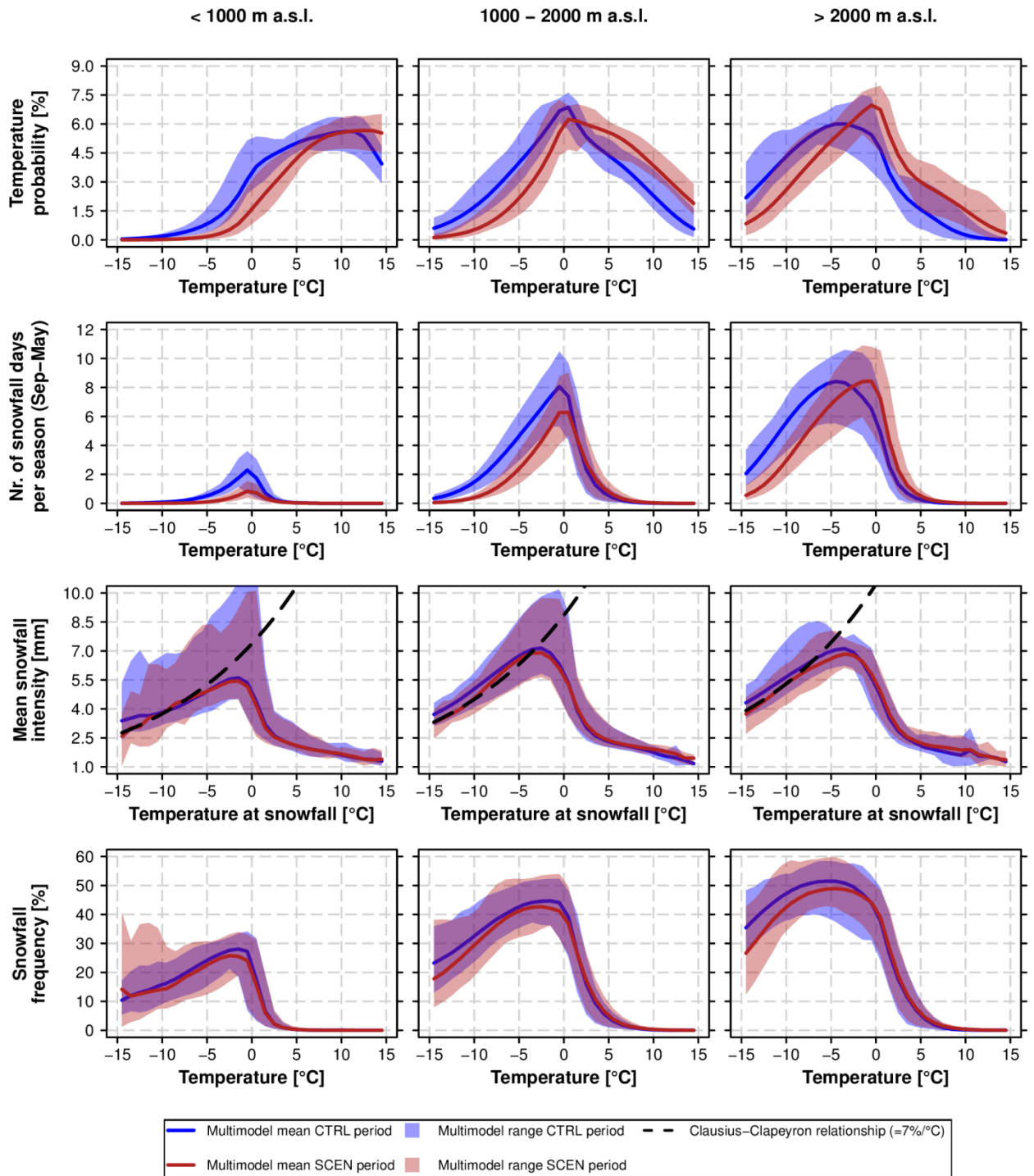
1329



1330
1331

1332 **Figure 9** Intercomparison of various snowfall indices and relationship with monthly mean temperature in CTRL.
 1333 For each panel, the monthly mean statistics for each 250 m elevation interval and for each of the 14 individual
 1334 GCM-RCM chains were derived (black circles). Red triangles denote the multi-model mean for a specific month
 1335 and elevation interval. The monthly statistics were calculated by considering all grid points of the specific
 1336 elevation intervals which are available for both variables in the corresponding scatterplot only (area consistency).
 1337 The data were taken from the 14 snowfall separated + bias-corrected-adjusted (RCM_{sep+bias}) RCM simulations.
 1338 Relative changes are based on the RCP8.5 driven simulations (SCEN 2070-2099 wrt. CTRL 1981-2010).

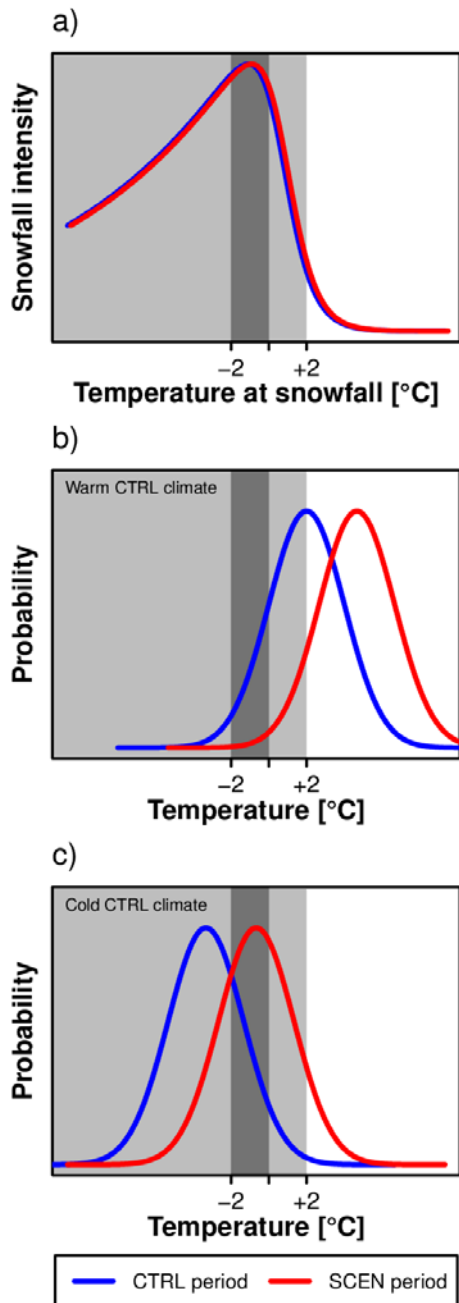
1339



1340

1341

1342 **Figure 10** Comparison of temperature probability, snowfall probability and mean snowfall intensity for the CTRL
1343 period 1981-2010 and SCEN period 2070-2099 for RCP8.5. The analysis is based on data from the 14 snowfall
1344 separated + bias-corrected-adjusted RCM simulations (RCM_{sep+bae}). The top row depicts the PDF of the daily
1345 temperature distribution, while the second row shows the mean number of snowfall days between September and
1346 May, i.e., days with $S > 1 \text{ mm/d}$ (see Tab. 2), in a particular temperature interval. The third row represents the
1347 mean snowfall intensity, S_{int} , for a given snowfall temperature interval. In addition the Clausius-Clapeyron
1348 relationship, centred at the -10°C mean S_{int} for SCEN, is displayed by the black dashed line. PDFs and mean S_{int}
1349 were calculated by creating daily mean temperature bins of width 1°C .



1350

1351

1352

1353

1354

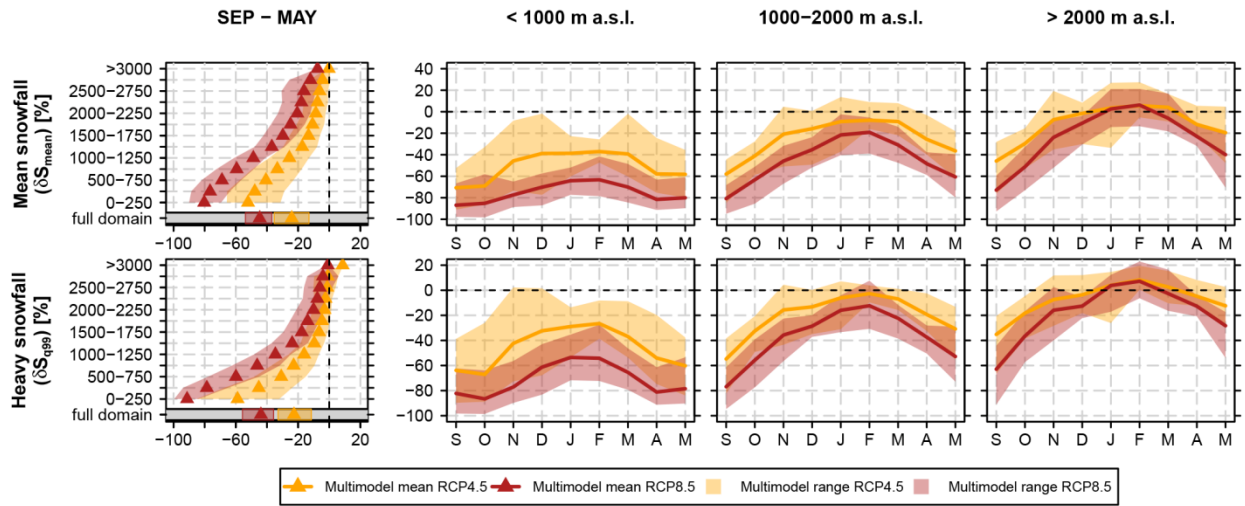
1355

1356

1357

1358

Figure 11 Schematic illustration of the control of changes in snowfall intensity on changes in mean and extreme snowfall. a) Relation between temperature and mean snowfall intensity. b) Daily temperature PDF for a warm control climate (low elevations or transition seasons, i.e., beginning or end of winter). c) Daily temperature PDF for a cold control climate (high elevations or mid-winter). The blue line denotes the historical CTRL period, the red line the future SCEN period. The light grey shaded area represents the overall temperature interval at which snowfall occurs, the dark grey shading shows the preferred temperature interval for heavy snowfall to occur.



1359

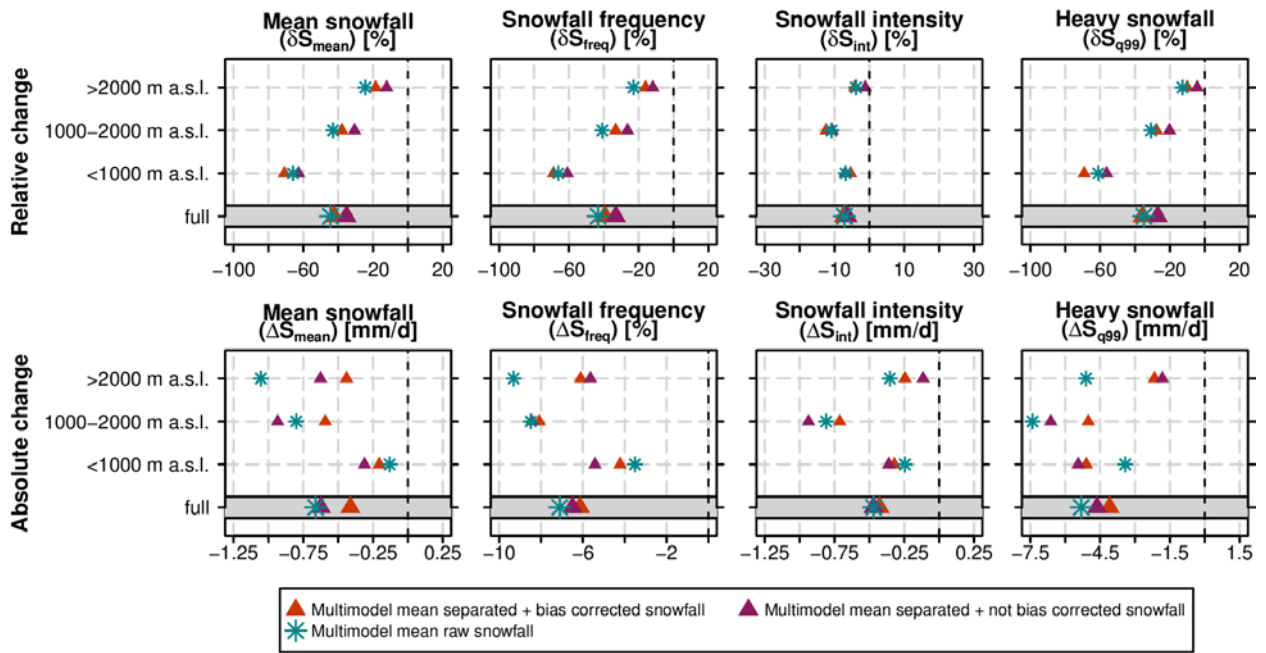
1360

1361

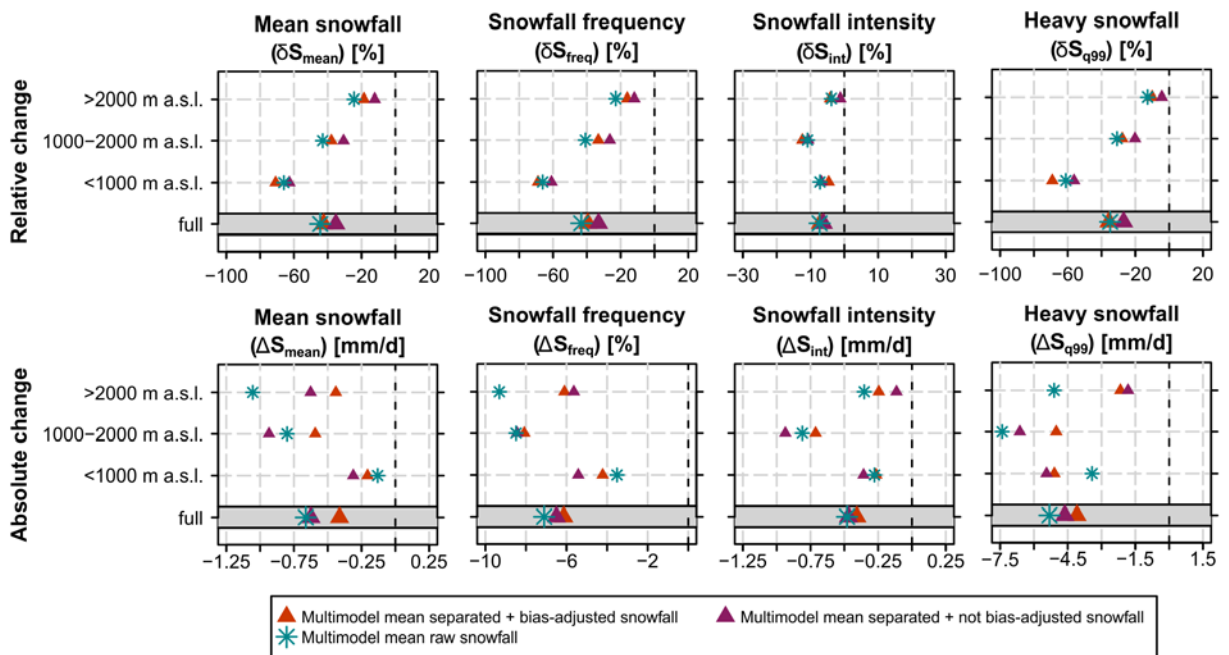
1362

1363

Figure 12 Similar as Figure 8 but showing projected changes of mean snowfall, δS_{mean} , and heavy snowfall, δS_{q99} , for the emission scenarios RCP4.5 and 8.5. See Fig. S98 for the emission scenario uncertainty of the remaining four snowfall indices.



1364
1365



1366
1367
1368
1369
1370
1371

Figure 13 Relative and absolute changes (SCEN period 2070-2099 with respect to CTRL period 1981-2010) of mean September-May snowfall indices based on a subset of 9 snowfall separated + bias-~~corrected~~-adjusted ($RCM_{sep+bae}$), 9 snowfall separated + not bias-~~corrected~~-adjusted ($RCM_{sep+nbae}$) and 9 raw snowfall RCM simulations (RCM_{raw}) for RCP8.5. Only RCM simulations providing raw snowfall as output variable (see Tab. 1) were used in this analysis.

1372

1373 **Tables**

1374

1375 | **Table 1** Overview on the 14 EURO-CORDEX simulations available for this study. The whole model set consists of
 1376 | seven RCMs driven by five different GCMs. All experiments were realized on a grid, covering the European
 1377 | domain, with a horizontal resolution of approximately 12.5 km (EUR-11) and were run for control RCP4.5 and
 1378 | RCP8.5 scenarios within the considered time periods of interest. A subset of 9 simulations provides raw snowfall,
 1379 | i.e., snowfall flux in kg/m²s, as output variable. For full institutional names the reader is referred to the official
 1380 | EURO-CORDEX website www.euro-cordex.net. Note that the EC-EARTH-driven experiments partly employ
 1381 | different realizations of the GCM run, i.e., explicitly sample the influence of internal climate variability in addition to
 1382 | model uncertainty.

RCM	GCM	Acronym	Institute ID	Raw snowfall output
ALADIN53	CNRM-CERFACS-CNRM-CM5	CNRM - ALADIN	CNRM	no
CCLM4-8-17	CNRM-CERFACS-CNRM-CM5	CNRM - CCLM	CLMcom/BTU	no
CCLM4-8-17	ICHEC-EC-EARTH	EC-EARTH - CCLM	CLMcom/BTU	no
CCLM4-8-17	MOHC-HadGEM2-ES	HadGEM2 - CCLM	CLMcom/ETH	no
CCLM4-8-17	MPI-M-MPI-ESM-LR	MPI-ESM - CCLM	CLMcom/BTU	no
HIRHAM5	ICHEC-EC-EARTH	EC-EARTH - HIRHAM	DMI	yes
RACMO22E	ICHEC-EC-EARTH	EC-EARTH - RACMO	KNMI	yes
RCA4	CNRM-CERFACS-CNRM-CM5	CNRM - RCA	SMHI	yes
RCA4	ICHEC-EC-EARTH	EC-EARTH - RCA	SMHI	yes
-RCA4	MOHC-HadGEM2-ES	HadGEM2 - RCA	SMHI	yes
RCA4	IPSL-IPSL-CM5A-MR	IPSL - RCA	SMHI	yes
RCA4	MPI-M-MPI-ESM-LR	MPI-ESM – RCA	SMHI	yes
REMO2009	MPI-M-MPI-ESM-LR	MPI-ESM – REMO*	MPI-CSC	yes
WRF331F	IPSL-IPSL-CM5A-MR	IPSL - WRF	IPSL-INERIS	yes

* r1i1p1 realisation

1383

1384

1385 **Table 2** Analysed snowfall indices. The last column indicates the threshold value in the CTRL period for
 1386 considering a grid cell in the climate changes analysis (grid cells with smaller values are skipped for the
 1387 respective analysis); first number: threshold for monthly analyses, second number: threshold for seasonal
 1388 analysis.

Index name	Acronym	Unit	Definition	Threshold for monthly / seasonal analysis
Mean snowfall	S_{mean}	mm	(Spatio-)temporal mean snowfall in mm snow water equivalent (only "mm" thereafter).	1 mm / 10 mm
Heavy snowfall	S_{q99}	mm/d	Grid point-based 99% all day snowfall percentile.	1 mm / 1 mm
Max. 1 day snowfall	S_{1d}	mm/d	Mean of each season's or month's maximum 1 day snowfall.	1 mm / 1 mm
Snowfall frequency	S_{freq}	%	Percentage of days with snowfall $S > 1$ mm/d within a specific time period.	1 % / 1 %
Snowfall intensity	S_{int}	mm/d	Mean snowfall intensity at days with snowfall $S > 1$ mm/d within a specific time period.	S_{freq} threshold passed
Snowfall fraction	S_{frac}	%	Percentage of total snowfall, S_{tot} , on total precipitation, P_{tot} , within a specific time period.	1 % / 1 %

1389
 1390
 1391
 1392